

NATIONAL ADVISORY COMMITTEE FOR AERONAUTICS

TECHNICAL NOTE 3615

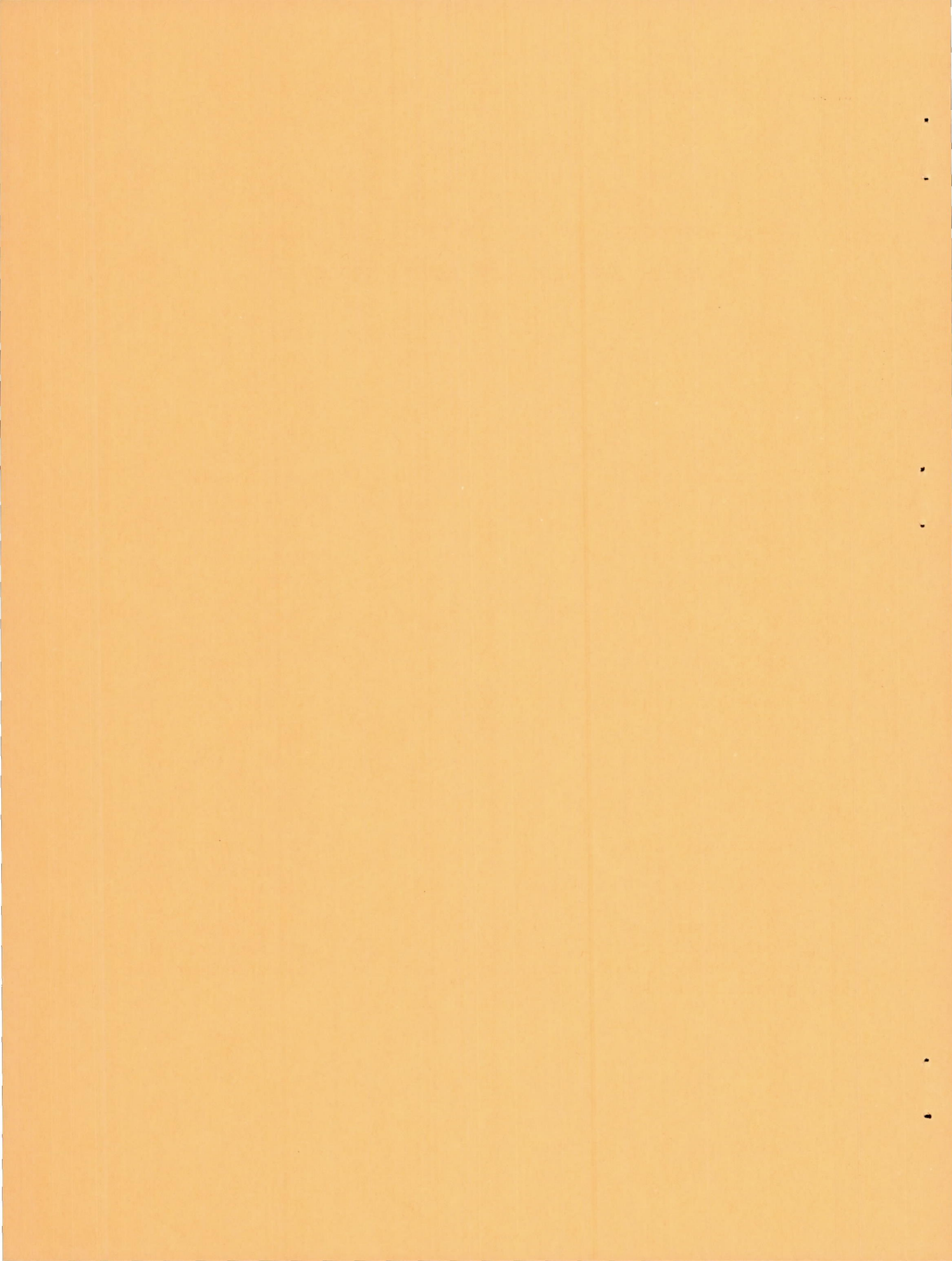
AN EXPERIMENTAL INVESTIGATION OF THE SCALE RELATIONS
FOR THE IMPINGING WATER SPRAY GENERATED BY
A PLANING SURFACE

By Ellis E. McBride

Langley Aeronautical Laboratory
Langley Field, Va.



Washington
February 1956



L
NATIONAL ADVISORY COMMITTEE FOR AERONAUTICS

TECHNICAL NOTE 3615

AN EXPERIMENTAL INVESTIGATION OF THE SCALE RELATIONS
FOR THE IMPINGING WATER SPRAY GENERATED BY
A PLANING SURFACE

By Ellis E. McBride

SUMMARY

An experimental investigation was made to determine the scale effects of the forces from water spray generated by a flat rectangular planing surface and impinging on a collector plate representative of an aerodynamic surface or other part of a water-based airplane. Lift and drag forces on the flat rectangular planing surface and on the spray-collector plate were measured. Underwater photographs of the wetted planing area and photographs of the spray generated by the planing surface were made. Two sizes of models were tested. The small model consisted of a flat rectangular planing surface with a 2-inch beam and a flat rectangular spray-collector plate 16 inches long and 10.67 inches wide. The large model was geometrically similar to the small model and was five times its linear dimensions. Tests were made with the collector plate in two vertical locations, 1.0 and 1.5 generator beams above the free water surface. The trim of the planing surface was set at 9°, 15°, and 20°, and wetted-length-beam ratios of 1.0, 1.5, 2.0, and 2.5 were tested at towing speeds from 10 to 80 feet per second.

The results of the investigation show that impinging-spray lift forces can be scaled by the conventional Froude relations. The small-model-spray drag forces, however, were found to be higher than those of the large model when scaled by the conventional Froude relations; thus, a Reynolds number effect on spray drag was indicated. By using an empirical method for correcting the spray friction drag coefficients on a Reynolds number basis, reasonable agreement with the Schoenherr line was generally obtained.

INTRODUCTION

In the past, seaplane spray investigations were primarily concerned with the definition and reduction of spray impinging on the propellers, horizontal-tail surfaces, and flaps because those regions of the aircraft were most susceptible to spray damage. Recent developments, however, have altered the spray consideration somewhat since modern seaplane designs utilize jet engines, low hulls, and auxiliary planing devices. These modern designs, therefore, have compact silhouettes with closely coupled aerodynamic and hydrodynamic components.

With aerodynamic surfaces constructed stronger to withstand high-speed flight loads, considerable forces may be developed on these surfaces by impinging spray without necessarily causing damage. These impinging-spray forces may be large enough to affect take-off performance, and whether there is a scale effect on them when model performance data are scaled to full size by the usual methods is therefore of interest.

In the present study the lift and drag forces on a flat collector plate caused by spray from a flat planing surface were investigated on two sizes of models in Langley tank no. 2. Comparisons of the results are given and an empirical method of correcting for the apparent Reynolds number effect obtained is suggested.

SYMBOLS

A	wetted area of spray collector, sq ft
b	beam of spray generator, ft
C_D	planing drag coefficient, $\frac{D}{\frac{\rho}{2} SV^2}$
$C_{D,s}$	spray drag coefficient, $\frac{D_s}{\frac{\rho}{2} SV^2}$
C_F	planing skin-friction drag coefficient, $C_D - C_L \tan \tau$
$C_{F,s}$	spray skin-friction drag coefficient, $\frac{D_s}{\frac{\rho}{2} AV^2 \sin^2(\alpha + \tau)}$

C_L	planing lift coefficient, $\frac{L}{\frac{\rho}{2} SV^2}$
$C_{L,s}$	spray lift coefficient, $\frac{L_s}{\frac{\rho}{2} SV^2}$
D	planing drag of spray generator, lb
D_s	spray drag of spray collector, lb
N_{Fr}	Froude number, $\frac{V}{\sqrt{gl}}$
g	acceleration of gravity, 32.2 ft/sec^2
L	planing lift of spray generator, lb
L_s	spray lift of spray collector, lb
l	wetted length of spray generator, ft
l_s	wetted length of spray collector, ft
R	Reynolds number of planing-surface flow, $\frac{Vl}{\nu}$
R_s	Reynolds number of spray flow, $\frac{V \sin(\alpha + \tau) l_s}{\nu}$
S	wetted area of spray generator, sq ft
V	carriage speed, fps
α	spray angle measured between leading edge of spray as it leaves chine of generator and free water surface, deg
ν	kinematic viscosity, ft^2/sec
ρ	density of tank water, for small model spray forces $\rho/2 = 0.971 \text{ slug/cu ft}$; for all others $\rho/2 = 0.984 \text{ slug/cu ft}$
τ	trim angle measured between bottom of planing surface and free water surface, deg

APPARATUS AND PROCEDURE

Description of Models

The models consisted of a spray generator and a spray collector. The spray generator was a flat rectangular planing plate. The spray collector was a flat rectangular plate which was mounted above and to the rear of the generator as shown in figure 1. The pertinent dimensions of the two models are listed in table I.

The large spray generator was constructed of mahogany laminations and was coated with white plastic. The small spray generator was constructed of one piece of mahogany and was coated on the bottom and sides with white plastic. The faces of the models were machined to a smooth surface and all corners and chines were sharp and square. The bottoms of the generators were marked off with grids to facilitate reading of wetted lengths from underwater photographs. The large collector plate was constructed of mahogany laminations coated with white plastic and was reinforced with two 3-inch steel channels running lengthwise to minimize deflection under load. The small collector plate consisted of one piece of clear plastic. The loads on this plate were too small to require external stiffening.

Test Methods and Equipment

The tests were made with the main towing carriage in Langley tank no. 2. The large model is shown attached to the towing carriage in figure 1(a). The spray generator was attached by means of a rigid strut to a two-component strain-gage balance capable of measuring 3,500 pounds of lift and 1,500 pounds of drag. The collector plate was attached to a similar two-component balance capable of measuring 1,000 pounds of lift and 250 pounds of drag. Each balance was provided with a shield to keep the spray from wetting the strain gages. Each balance fed into a separate two-channel strip-chart recorder.

The small model is shown attached to the towing carriage in figure 1(b). The spray generator was attached to the small-model towing gear in Langley tank no. 2. Lift and drag were measured by electrical strain-gage beams and the deflections were read visually on galvanometers. The collector plate was attached to a special balance shown covered by a spray-shield box in figure 1(b). A thin rubber diaphragm was used as a seal between the plate and box and offered no appreciable restraint to the deflection of the strain gages. Figure 1(c) is a photograph of this balance with the spray shield removed. The lift and drag on the spray collector were measured by two single-component strain-gage load cells mounted at right angles to each other. The lift load cell was

capable of measuring 5 pounds and the drag cell 3 pounds. The load cells fed into a two-channel strip-chart recorder.

Underwater photographs were made with a 70-millimeter camera mounted in a waterproof box located on the bottom of the tank. The camera and high-speed flash lamps were set off by the action of the carriage interrupting a photoelectric beam. Photographs of the spray were made by a similar camera mounted on a boom attached to the towing carriage.

The accuracy of the various balances and recording devices was considered to be as follows:

Tests were made at generator trims of 9° , 15° , and 20° at wetted-length-beam ratios of 1.0, 1.5, 2.0, and 2.5. The collector plate was tested at 0° trim in two vertical locations, 1.0 and 1.5 generator beams above the free water surface. Constant-speed runs were made from 10 to 80 feet per second with both models. Small-model spray-collector forces, however, were measured only up to 35 feet per second since this speed compares on a Froude basis with about 80 feet per second on the large model.

The measurements were made without a wind screen. Aerodynamic tares were measured and subtracted from all the data presented.

Data Reduction

The wetted area of the spray generator was measured from the under-water photographs. Because of structural deflections caused by the forces on the models, the wetted lengths and trims could not be preset as accurately as desired; therefore, a certain amount of cross-plotting was required. The planing lift and drag in pounds were plotted against the measured wetted areas, with speed and desired trim as parameters. From these plots, data at the desired length-beam ratios were read and cross-plotted against true trim. The true trim was computed from the measured forces and the corresponding trim changes obtained during the balance calibrations. From the cross plots the planing lift and

drag at the desired wetted-length-beam ratio, trim, and speed were obtained. These data were reduced to coefficient form by the

relationships $C_L = \frac{L}{\frac{\rho}{2} SV^2}$ and $C_D = \frac{D}{\frac{\rho}{2} SV^2}$. The skin-friction coefficient

for the generator was computed by the relation $C_F = C_D - C_L \tan \tau$.

The spray forces on the large model were handled in a manner similar to that used for the planing forces. The measured spray lift and drag forces obtained with the collector plate were plotted against the wetted area of the generator. Then cross plots against true generator trim were made. The small-model test equipment was such that the spray forces could be obtained by setting the desired trim and wetted length accurately; thus, fairing and cross-plotting were not necessary. The spray lift and drag forces were reduced to coefficient form based on the generator wetted area by the following relationships:

$$C_{L,s} = \frac{L_s}{\frac{\rho}{2} SV^2}$$

$$C_{D,s} = \frac{D_s}{\frac{\rho}{2} SV^2}$$

RESULTS AND DISCUSSION

Analysis of Planing Data

Figure 2 shows typical underwater photographs of the spray generator. The planing lift coefficients obtained with both the large and small generators are shown in figure 3, along with curves based on the theory of Shuford (ref. 1). The test data of the two models are in good agreement with each other and are in reasonable agreement with the theory.

The skin-friction portion of the total drag measured at 9° trim is plotted against Reynolds number along with the Blasius laminar line and the Schoenherr turbulent line (ref. 2) in figure 4. This plot indicates that in the low-speed range the small-model boundary layer was laminar. At higher speeds the boundary layer was transitional from laminar to turbulent. At the highest Reynolds numbers obtained, the boundary layer

became fully turbulent. The boundary layer of the large model was turbulent throughout the entire speed range and very good agreement with the Schoenherr fully turbulent line was obtained.

At trims of 15° and 20° the effect of Reynolds number on the total drag was negligible, as would be expected. At low trims, however, proper consideration of the Reynolds number effect on the skin friction must, of course, be made in order to scale the small-model data with the best accuracy possible.

Analysis of Spray Data

Figure 5 shows photographs of the small-model spray. Figure 6 shows photographs of the large-model spray.

The spray angle α for representative conditions measured from photographs such as shown in figure 5 is plotted in figure 7. The spray angle was measured between the leading edge of the spray as it left the chine of the generator and the free water surface. It was measured from the small-model photographs only but must be representative of the large model also since the two flows are similar as is shown subsequently. The trim of the generator was found to be the primary parameter governing the spray angle and the maximum vertical height of the spray. The spray angle increased rapidly with increasing speed and then became constant at speeds above about 22.5 feet per second. The speed at which the spray angle becomes constant may be taken as an additional parameter for establishing the speed at which the plate is fully planing.

Representative spray lift and spray drag coefficients are plotted against Froude number in figures 8 to 12. The best value of L/D obtained on the collector plate was less than 2.5; hence, the spray impinging on an aerodynamic surface can seriously reduce the value of L/D of a water-based airplane.

The spray force coefficients plotted in figures 8 to 12 are based on the generator wetted area in order to compare the spray force coefficients for the two models at like planing conditions. The spray lift coefficients obtained with the small model agree with those of the large model. Since these lift coefficients are in agreement, the two flows are assumed to be similar; that is, both the dynamic pressure of the spray $\frac{\rho}{2} V^2$ and the wetted area of the collector plate can be scaled according to Froude. The drag coefficients of the small model, however, were consistently higher than those of the large model.

The lift of the collector plate is determined essentially by the upward momentum of the spray that strikes it and the (probably much smaller) downward momentum of the spray that rebounds from it. The absence of scale effect on the lift coefficient thus implies that the spray pattern and the momentum transfer are determined mainly by the Froude number and are largely independent of Reynolds number. The drag, however, is exclusively skin friction between the collector and the fluid that runs along it and is apparently subject to the usual scale effect.

An effort was made to correlate the measured drag with the usual laws of skin friction. Any such correlation, of course, would be empirical, since both the velocity and the physical characteristics (such as density and viscosity) of the foamy mixture that runs along the collector would hardly be well defined. A fair correlation was achieved, however, on the basis of the following assumptions concerning the flow along the plate:

ρ_s density of spray (assumed equal to density ρ of water in the tank)

ν_s kinematic viscosity of spray (assumed equal to kinematic viscosity ν of water in the tank)

v_s spray velocity, $V \sin(\tau + \alpha)$

l_s wetted length of collector plate (defined by assuming that the spray continues at the initial spray angle α (fig. 5) until it meets the collector plate)

A wetted area of spray collector; defined as the product of the collector width and the wetted length l_s (actually, the entire width of the collector was not wetted at the lowest trim angle and the largest height of the collector above the water.)

The spray friction drag coefficients and Reynolds numbers were computed, according to these assumptions, as

$$C_{F,s} = \frac{D_s}{\frac{\rho}{2} A V_s^2}$$

$$R_s = \frac{V_s l_s}{\nu}$$

The experimental variation of spray friction drag coefficient with Reynolds number is shown in figures 13 to 17 along with the Schoenherr turbulent skin-friction line. Reasonable agreement with the Schoenherr line was obtained. In some cases the data fall slightly higher or lower than the Schoenherr line but, in general, are still parallel to this line. This discrepancy is probably due to the rather inaccurate method of determining the wetted area of the collector plate.

This analysis indicates that the scale effect on the tangential force due to spray is primarily that due to the variation in skin friction with Reynolds number and hence can be appreciable. If it is desirable to correct for this scale effect, certain observations and measurements are required to establish the effective Reynolds number and friction coefficients associated with the areas wetted by the spray. The method used in this paper, although empirical, will result in a closer approximation of the full-scale drag than could be obtained by scaling the total model drag by the Froude relations. Any method which satisfactorily relates the spray drag and Reynolds number would be sufficient.

CONCLUSIONS

An experimental investigation was made to determine the scale effects of the forces from water spray generated by a flat rectangular planing surface and impinging on a collector plate representative of an aerodynamic surface or other part of a water-based airplane. From the results of this investigation, the following conclusions were drawn:

1. It was found that impinging-spray lift forces could be scaled by the conventional Froude relations. The small-model spray drag forces, however, were found to be higher than those of the large model when scaled by the conventional Froude relations; thus, a Reynolds number effect on the spray drag was indicated.
2. By using an empirical method for correcting the spray friction drag coefficients on a Reynolds number basis, reasonable agreement with the Schoenherr line was generally obtained.

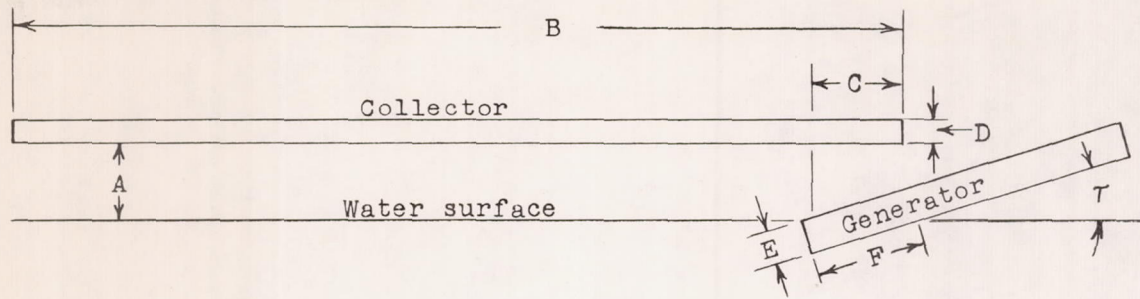
Langley Aeronautical Laboratory,
National Advisory Committee for Aeronautics,
Langley Field, Va., October 31, 1955.

REFERENCES

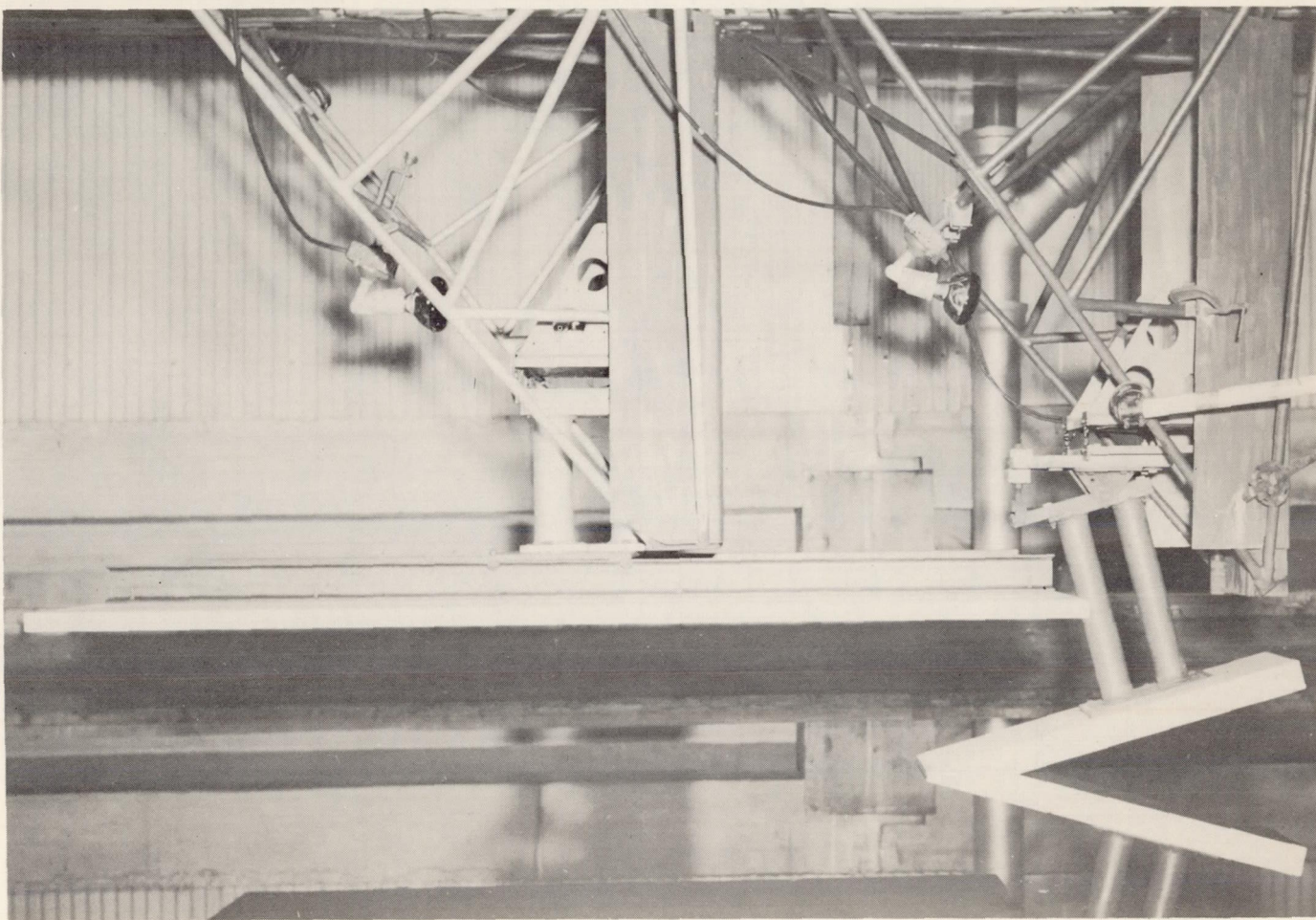
1. Shuford, Charles L., Jr.: A Review of Planing Theory and Experiment With a Theoretical Study of Pure-Planing Lift of Rectangular Flat Plates. NACA TN 3233, 1954.
2. Davidson, Kenneth S. M.: Resistance and Powering. Detailed Considerations - Skin Friction. Vol. II of Principles of Naval Architecture, ch. II, pt. 2, sec. 7, Henry E. Rossell and Lawrence B. Chapman, eds., Soc. Naval Arch. and Marine Eng., 1939, pp. 76-83.

TABLE I
PERTINENT MODEL DIMENSIONS AND TEST PARAMETERS

[All dimensions are in inches. Large generator beam, 10 inches; large collector beam, 53.3 inches; small generator beam, 2 inches; small collector beam, 10.67 inches]



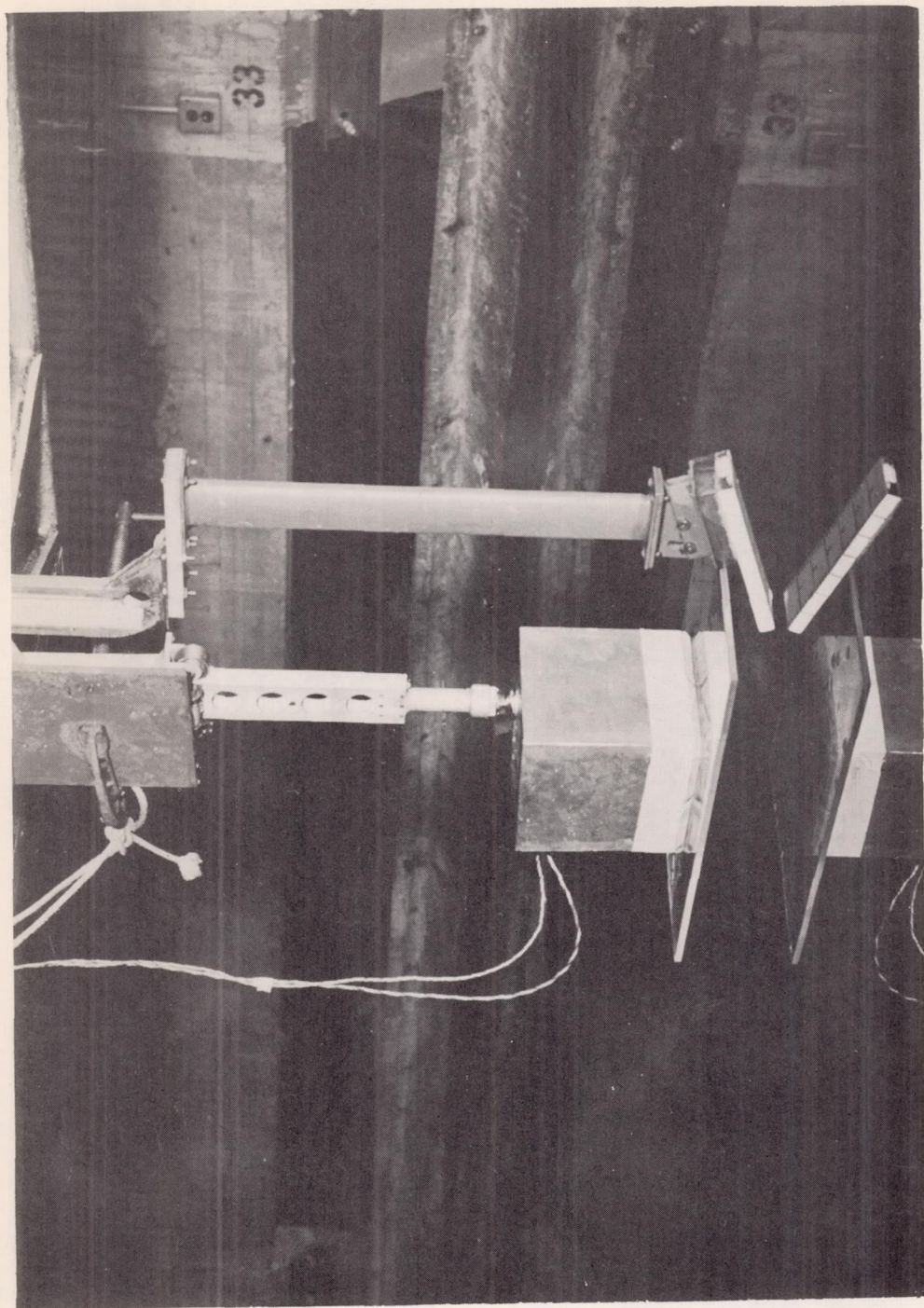
Dimensions	Large	Small	Large	Small	Large	Small
	$\tau = 9^\circ$		$\tau = 15^\circ$		$\tau = 20^\circ$	
A	10 15	2.0 3.0	10 15	2.0 3.0	10 15	2.0 3.0
B	80	16	80	16	80	16
C	12.65	2.53	10.35	2.07	8.15	1.63
D	1.25	0.25	1.25	0.25	1.25	0.25
E	2.5	0.5	2.5	0.5	2.5	0.5
F	10	2.0	10	2.0	10	2.0
	15	3.0	15	3.0	15	3.0
	20	4.0	20	4.0	20	4.0
	25	5.0	25	5.0	25	5.0



(a) Large model.

L-90540

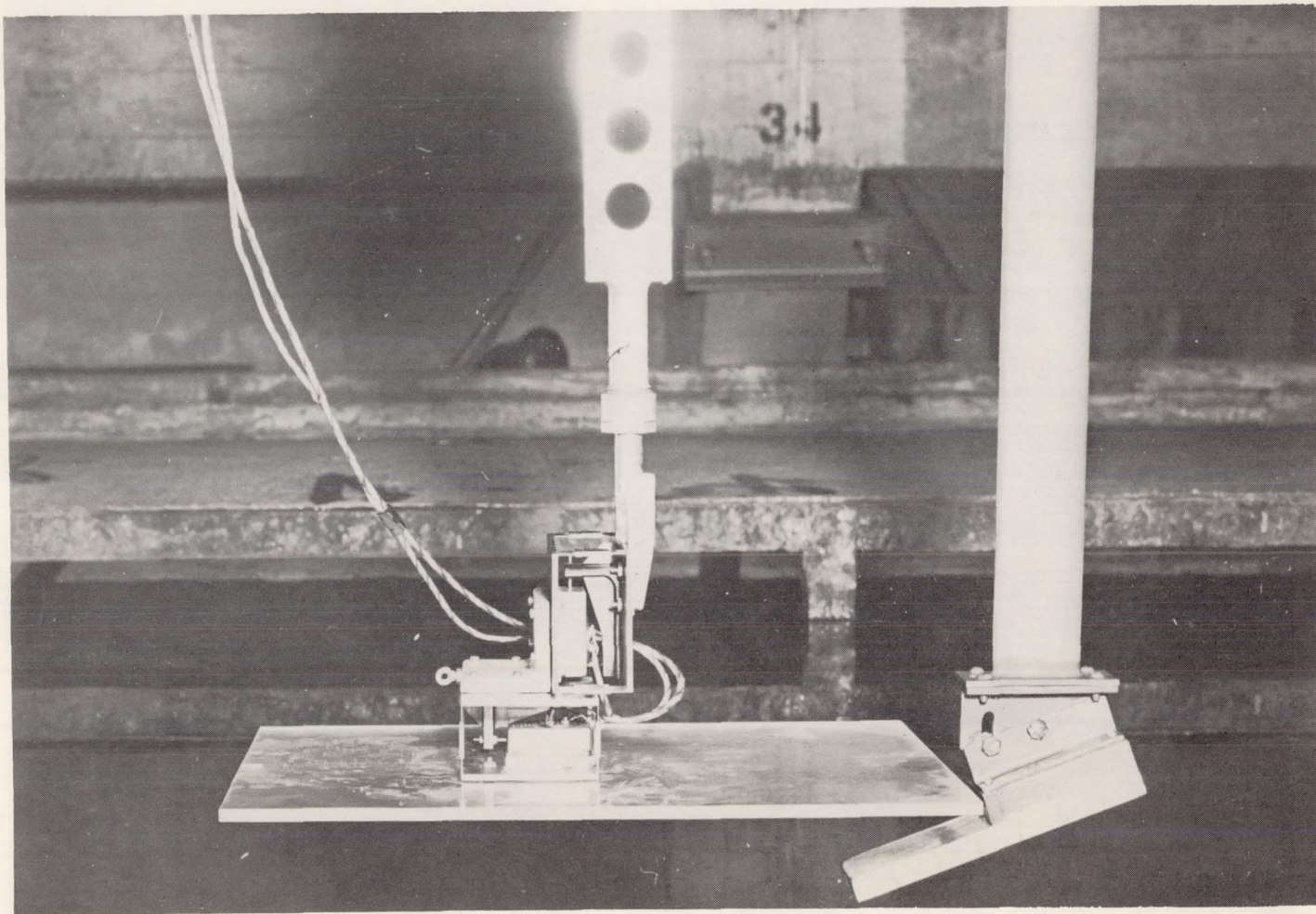
Figure 1.- Photographs of models and test equipment installed on towing carriage.



L-90541

(b) Small model.

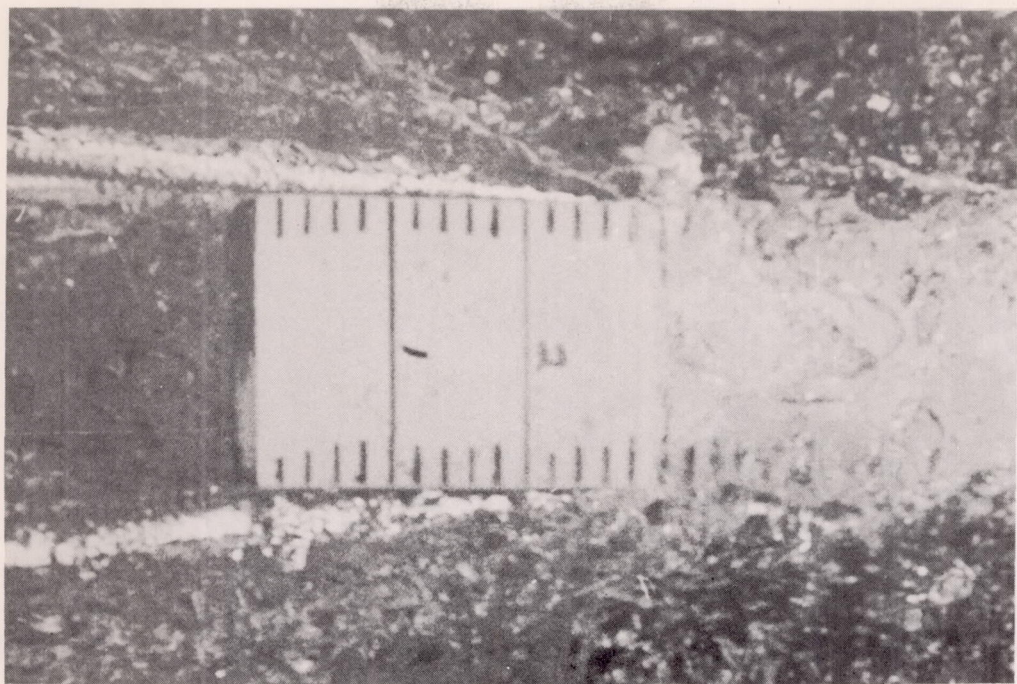
Figure 1.- Continued.



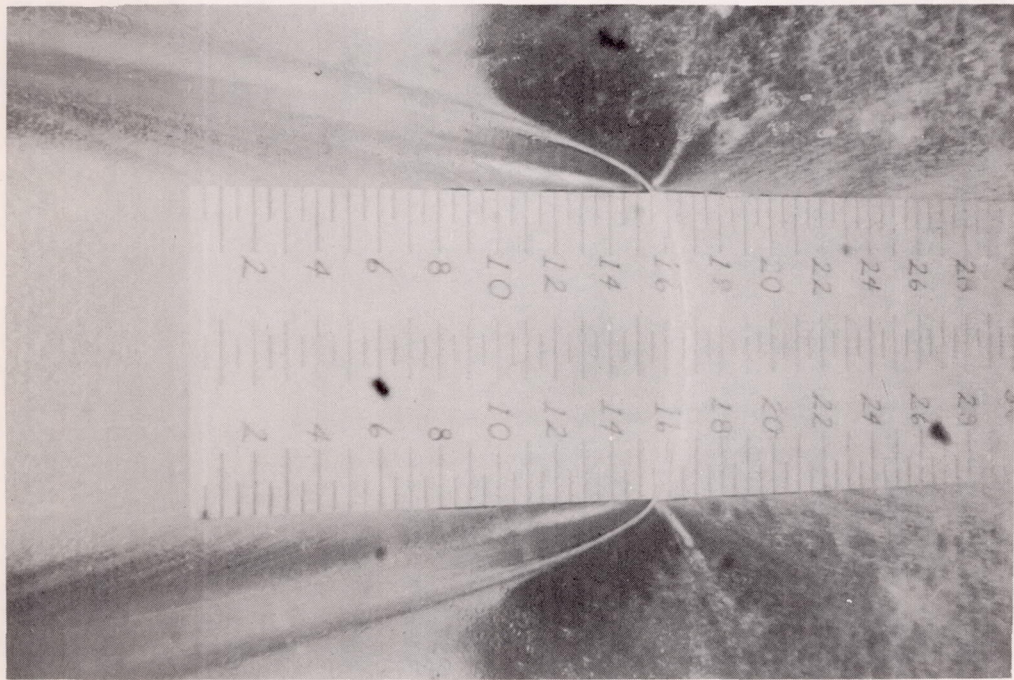
(c) Small model with spray shield removed.

L-90542

Figure 1.- Concluded.



(a) Small model.



(b) Large model.

L-90543

Figure 2.- Typical underwater photographs.

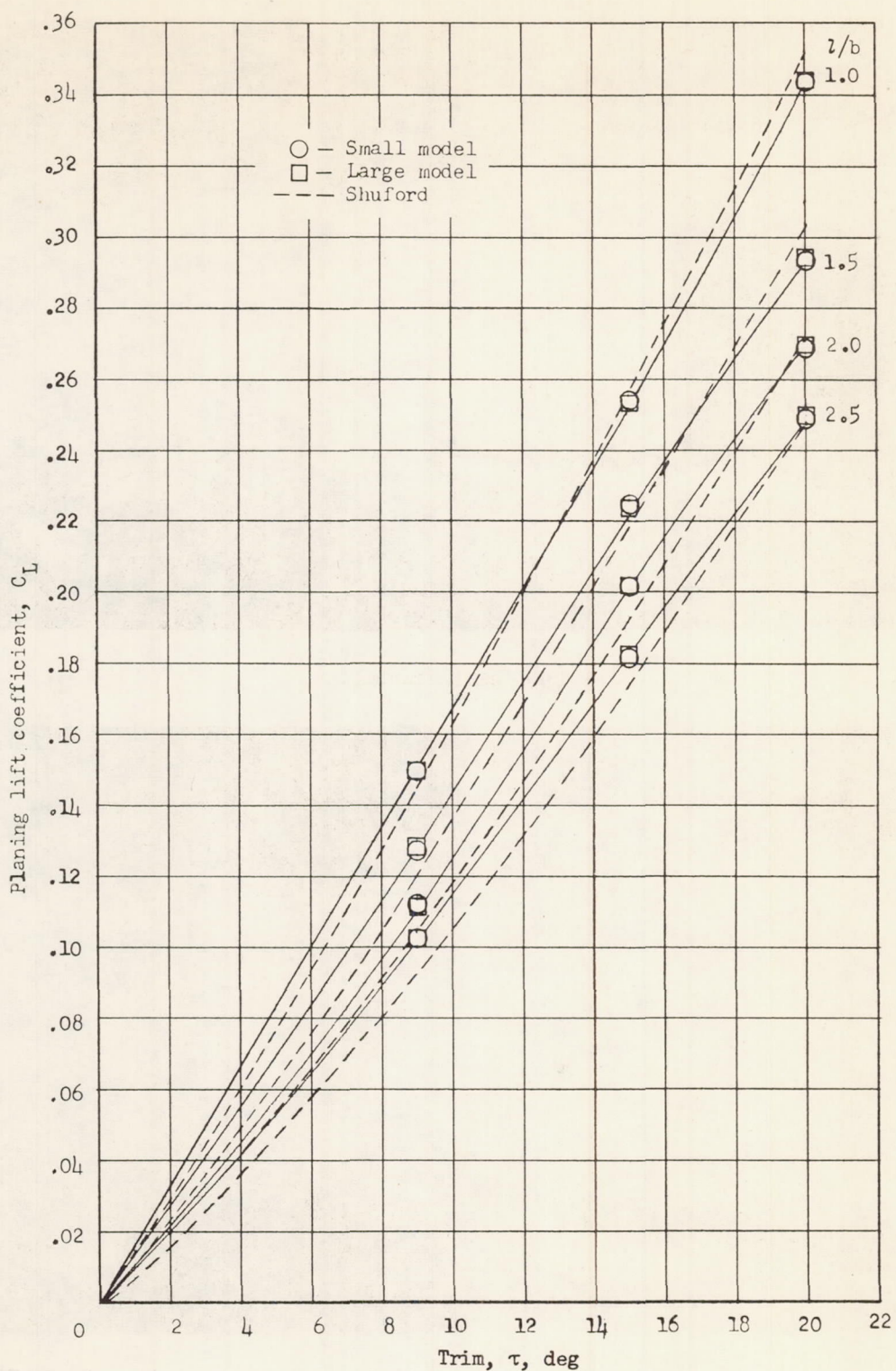


Figure 3.- Comparison of large- and small-model planing lift coefficients with the theory of Shuford (ref. 1).

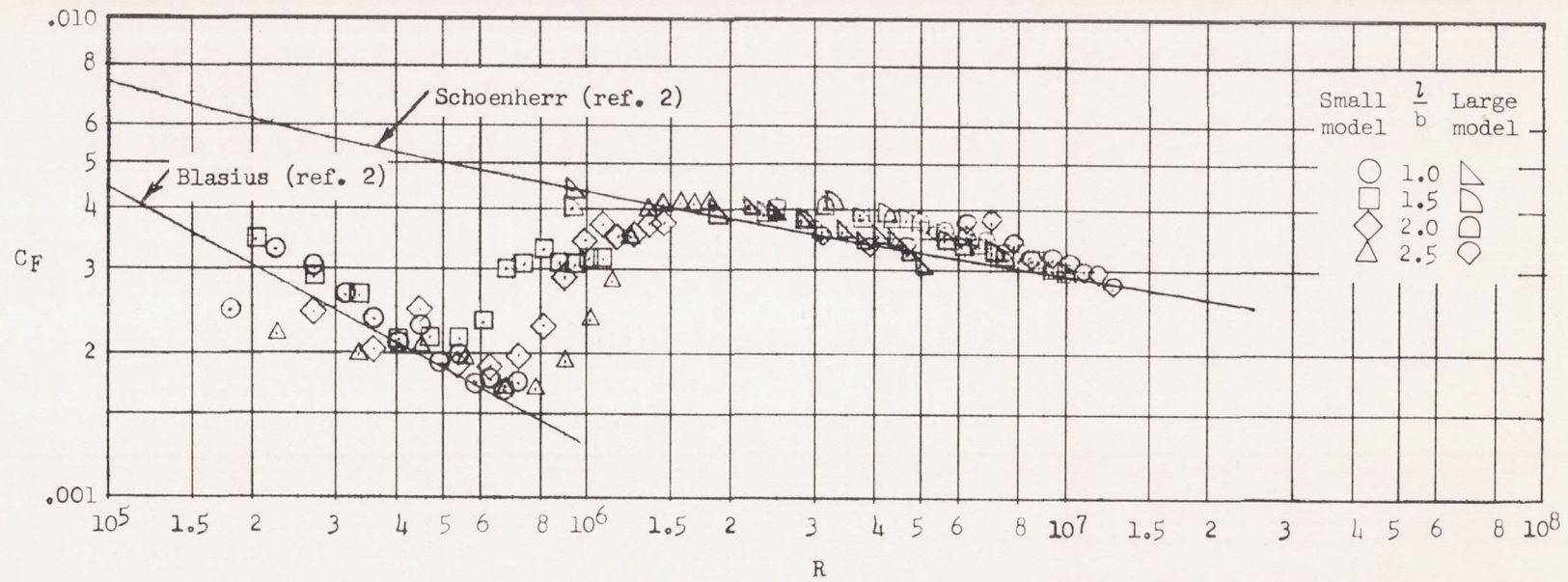
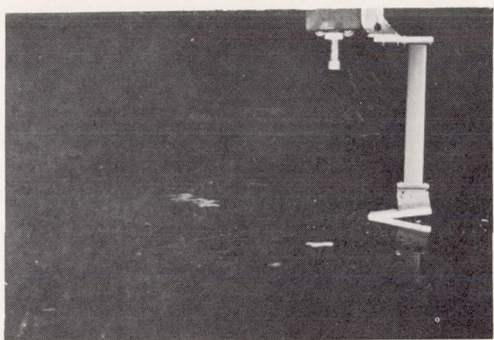
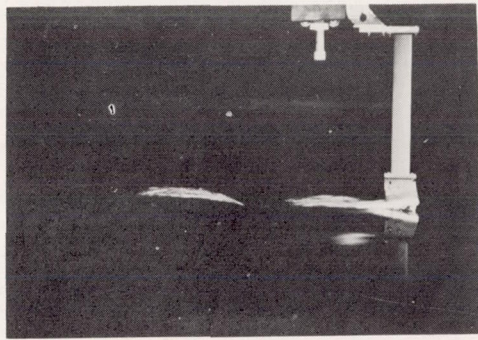


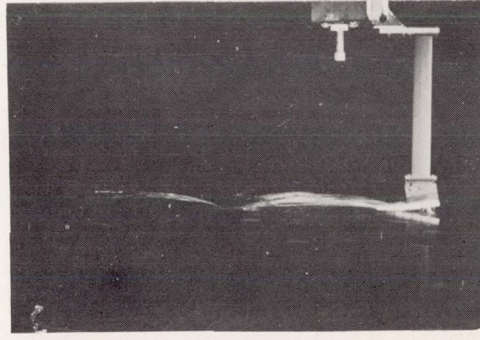
Figure 4.- Variation of large- and small-model skin-friction coefficients with Reynolds number. $\tau = 9^\circ$.



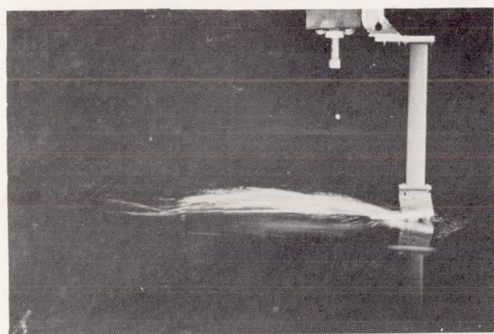
0 fps



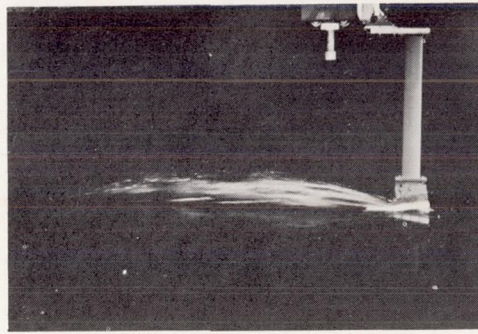
10 fps



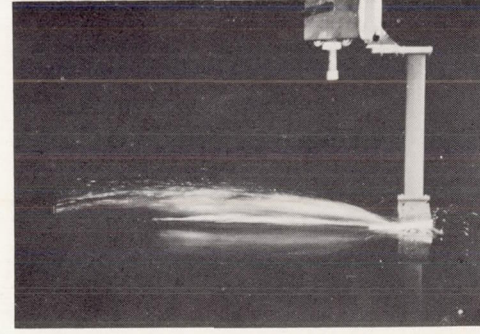
12.5 fps



15 fps



17.5 fps



20 fps

L-90544

Figure 5.- Spray photographs of the small model with the collector plate removed.

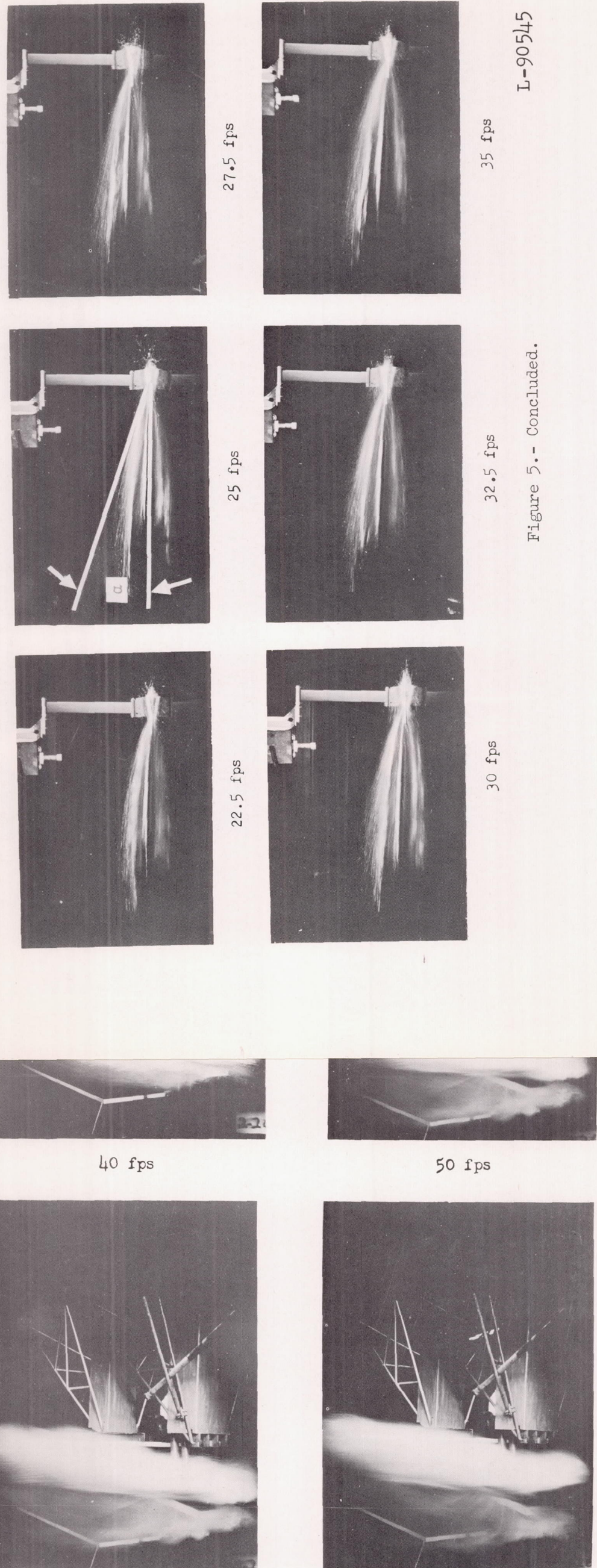


Figure 5.- Concluded.

L-90547

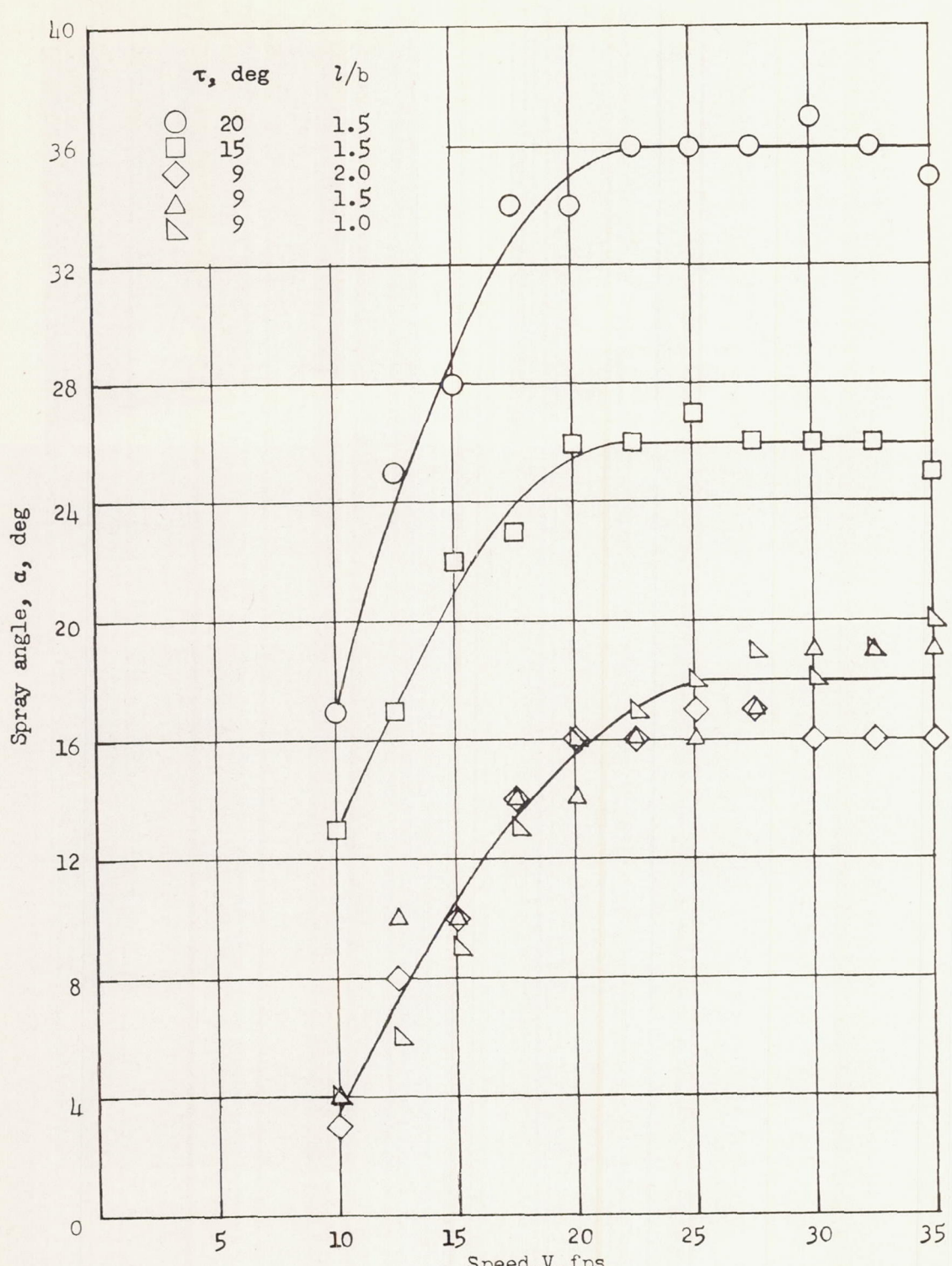
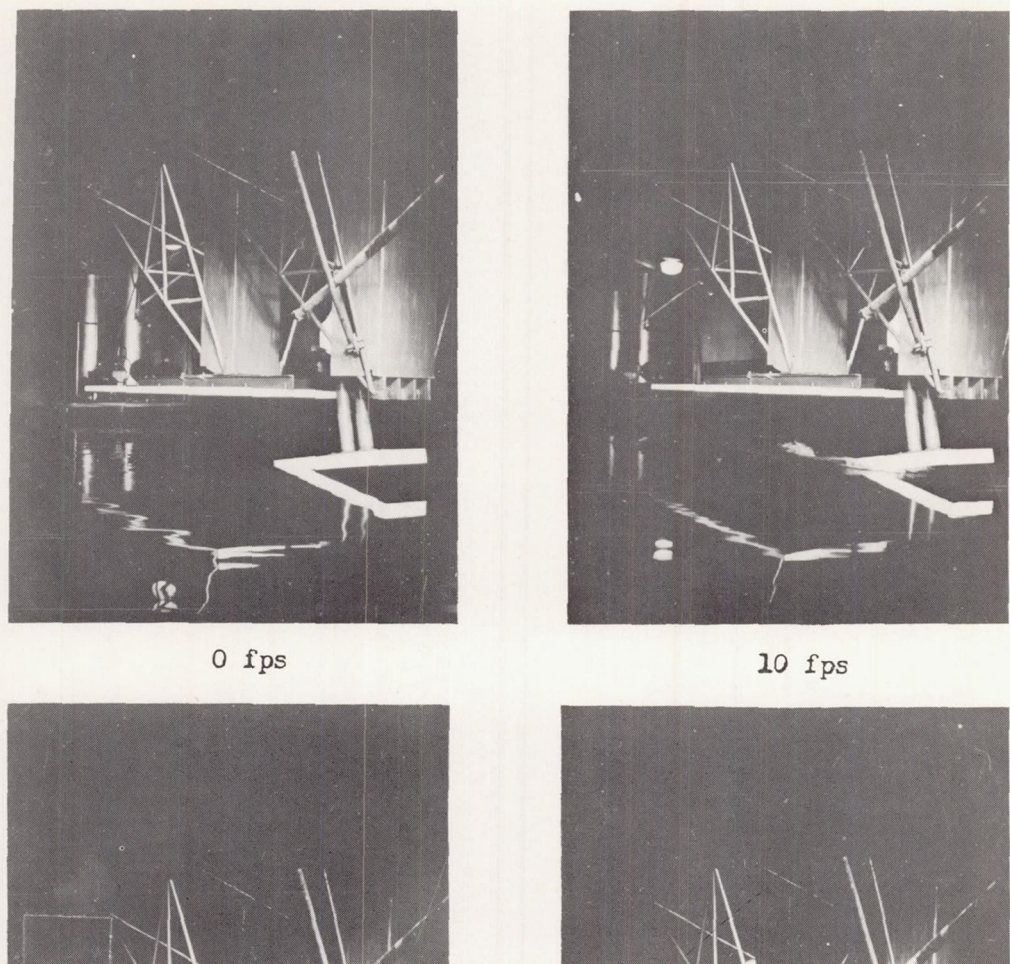
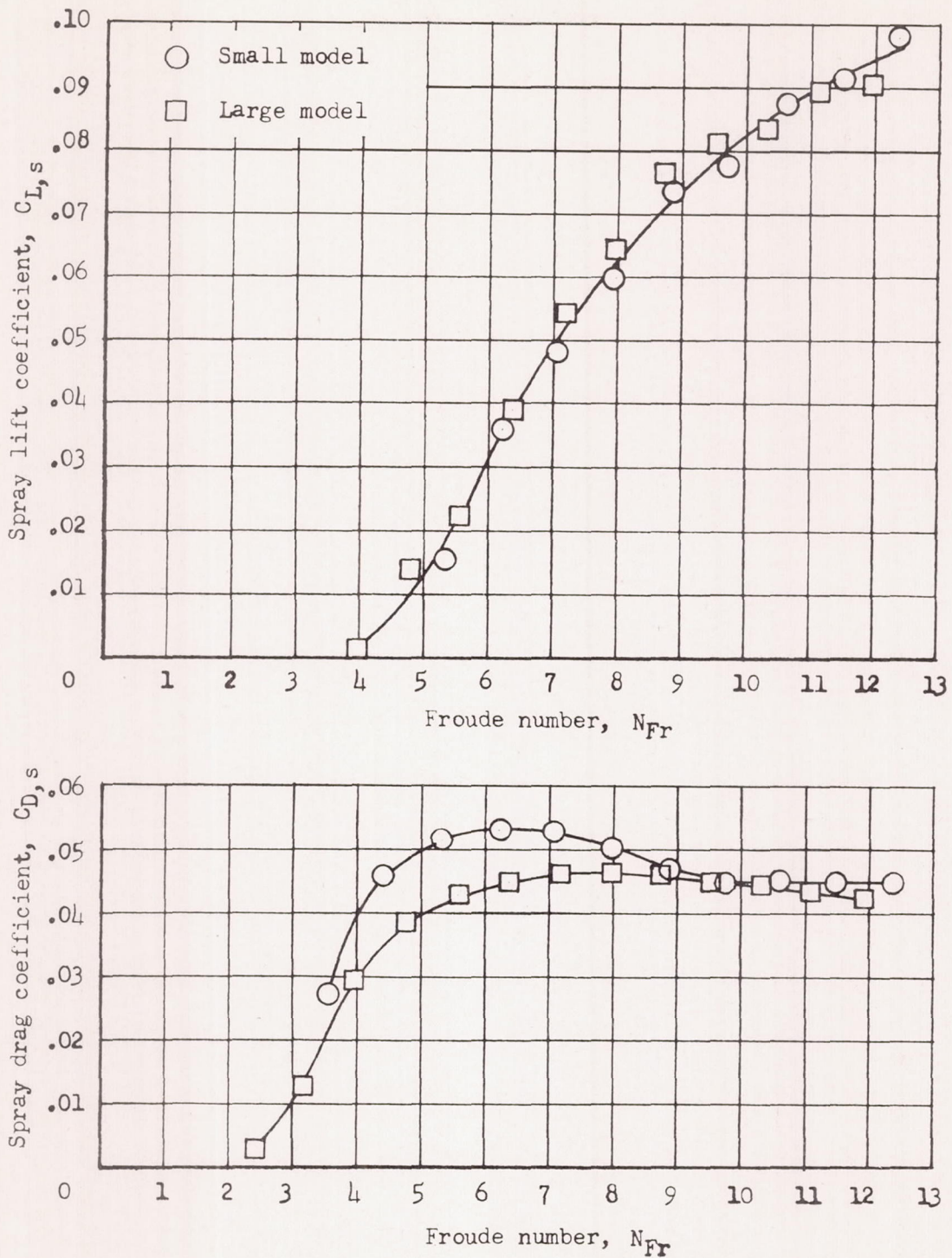
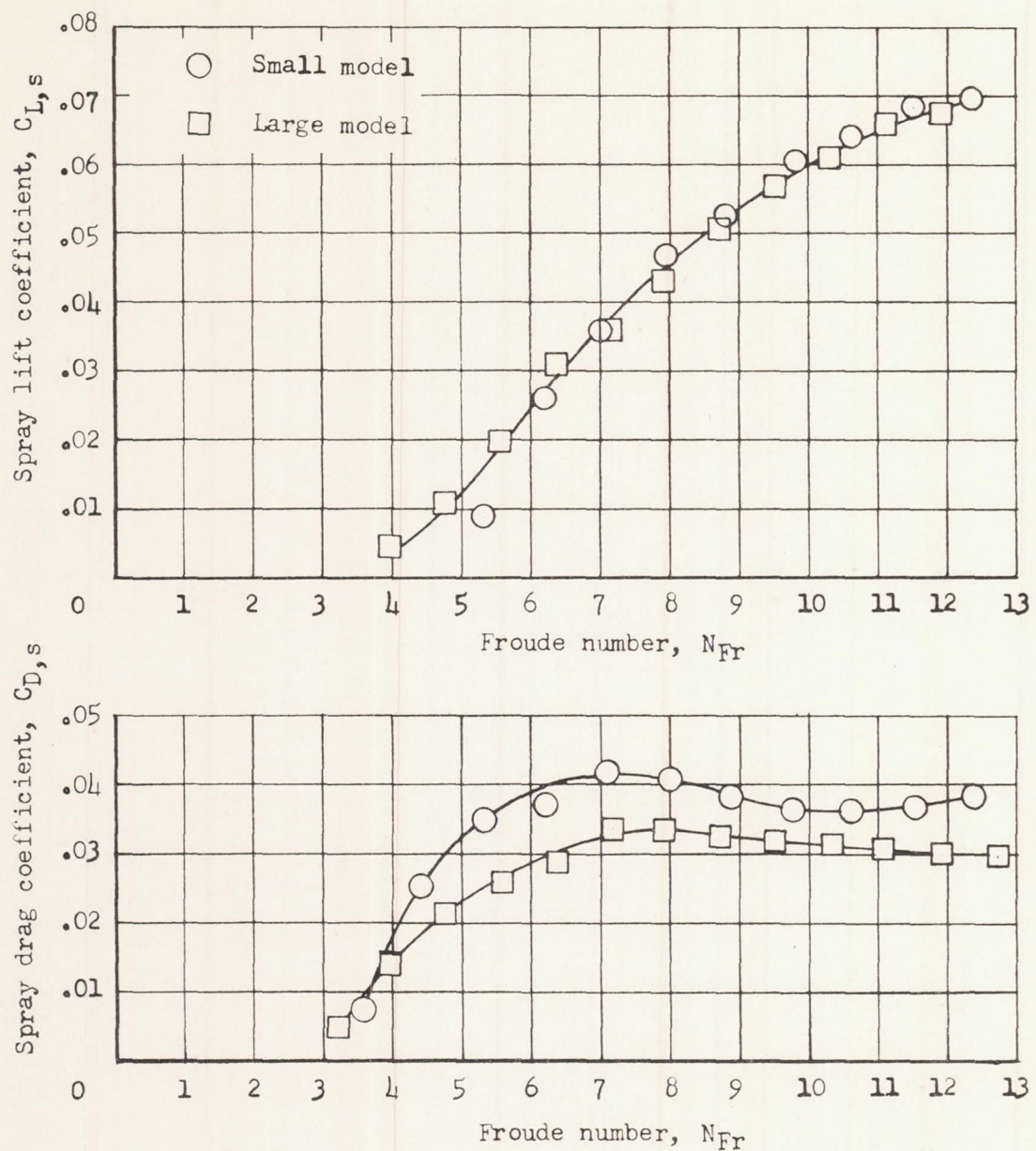


Figure 7.- Variation of spray angle with speed. Small-model data.



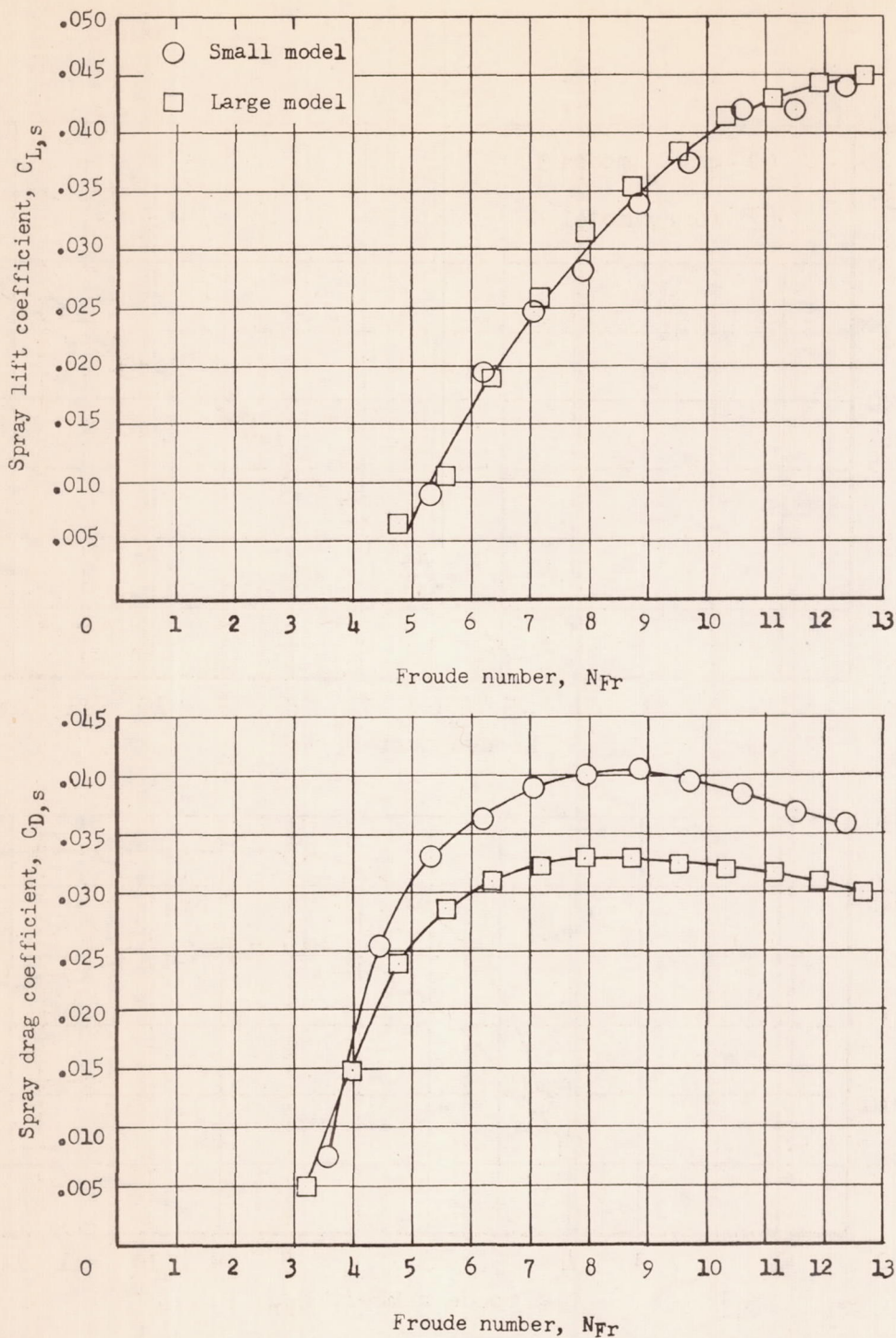
(a) Collector height, 1.0 beam.

Figure 8.- Variation of spray lift and drag coefficients with Froude number. $\tau = 20^\circ$; $l/b = 1.5$.



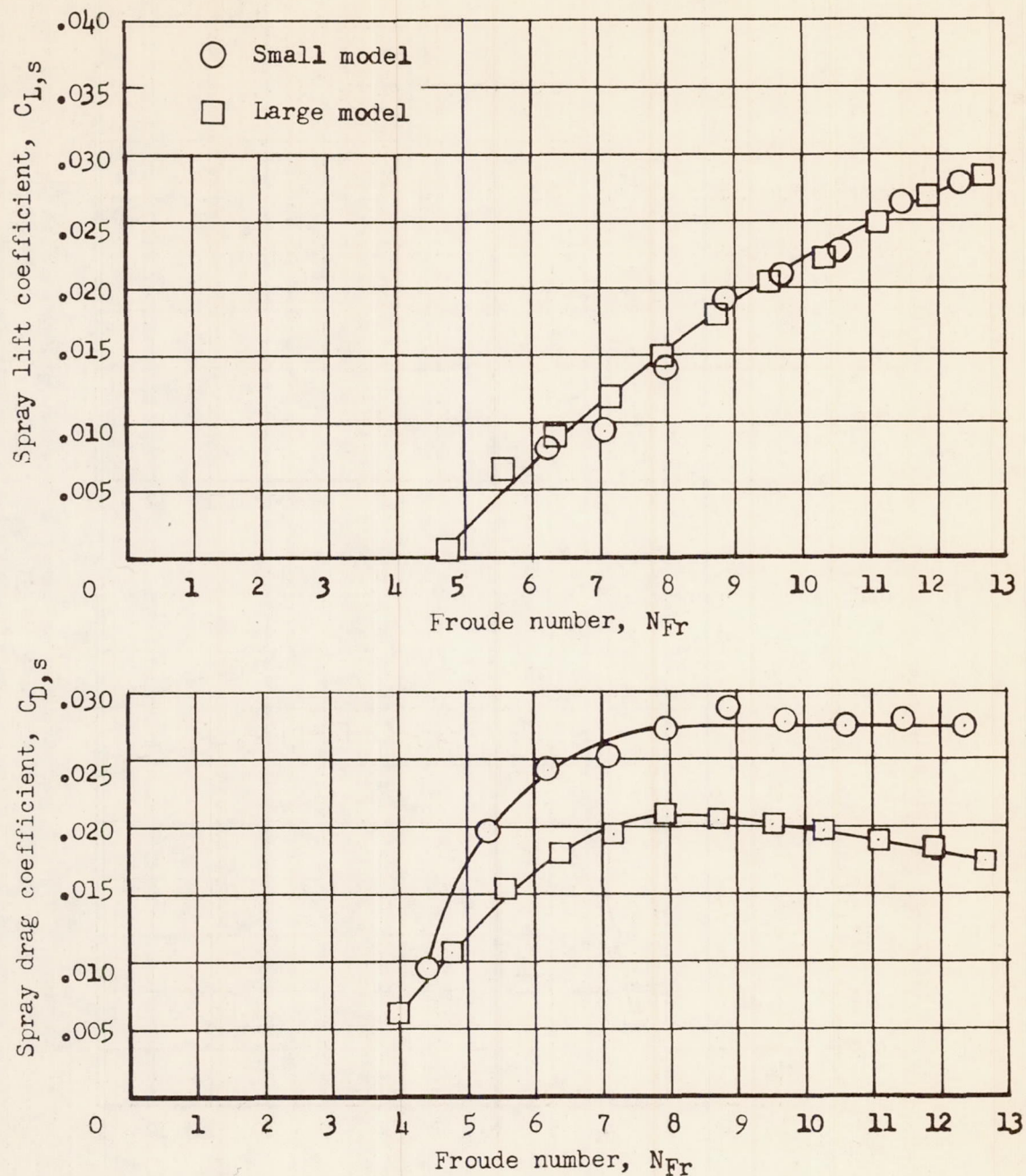
(b) Collector height, 1.5 beams.

Figure 8.- Concluded.



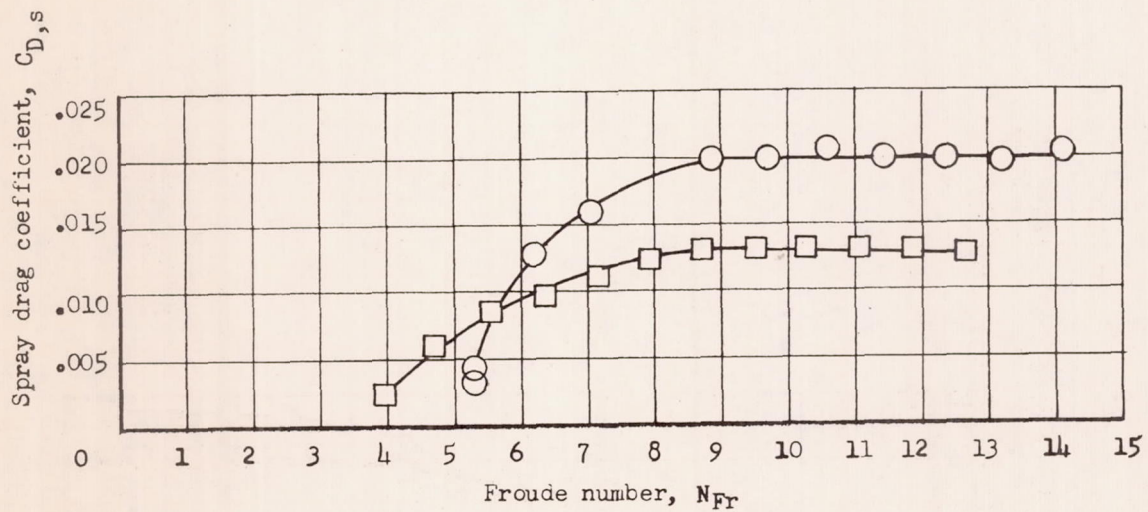
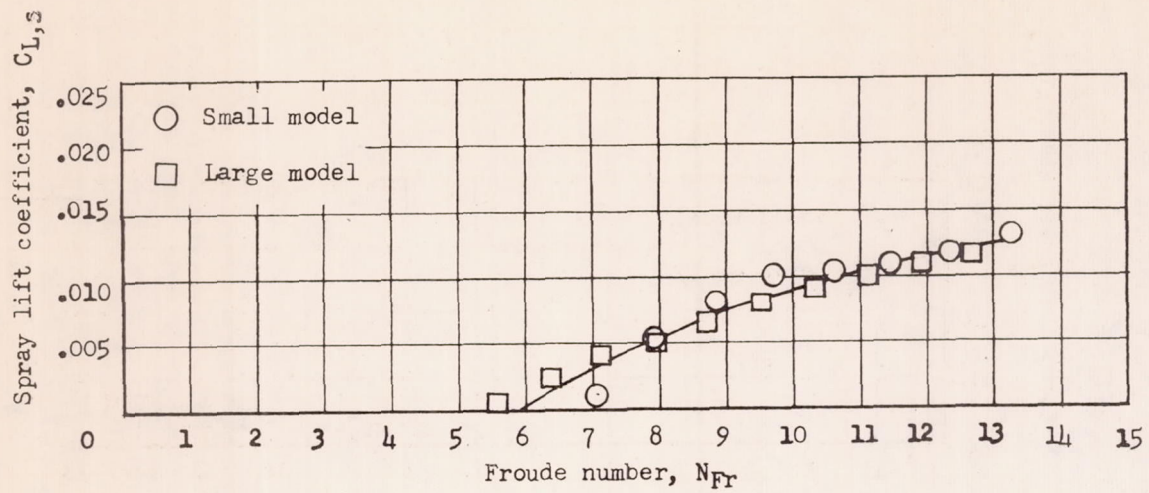
(a) Collector height, 1.0 beam.

Figure 9.- Variation of spray lift and drag coefficients with Froude number. $\tau = 15^\circ$; $l/b = 1.5$.



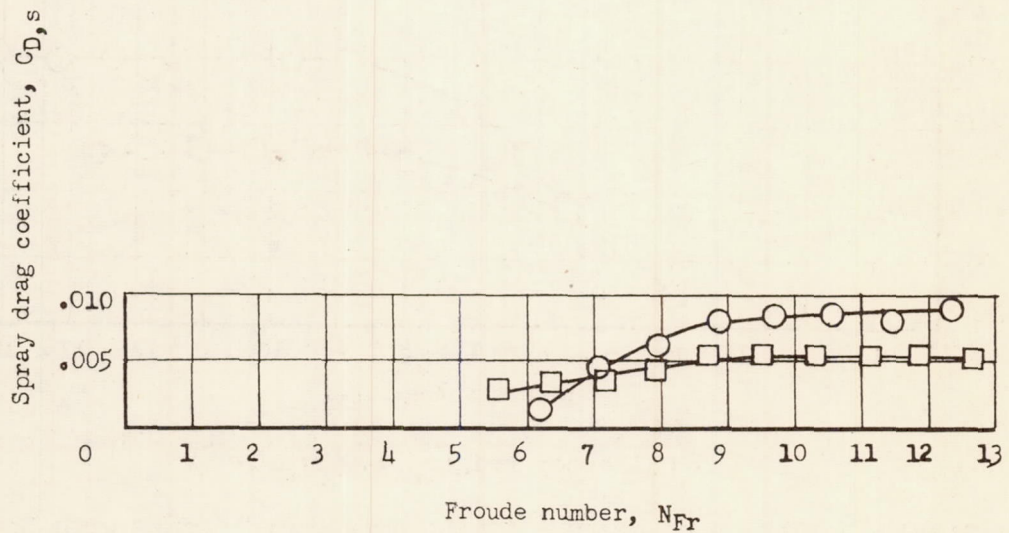
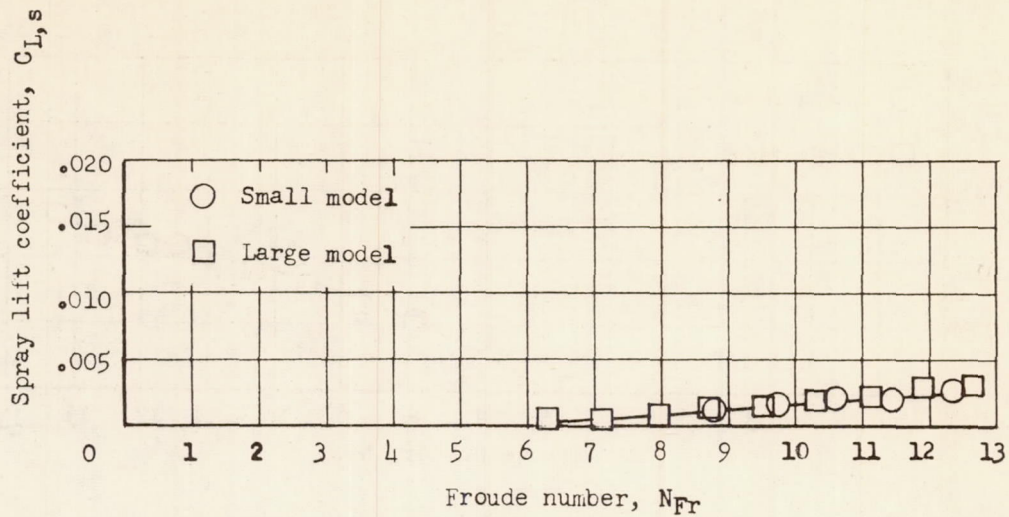
(b) Collector height, 1.5 beams.

Figure 9.- Concluded.



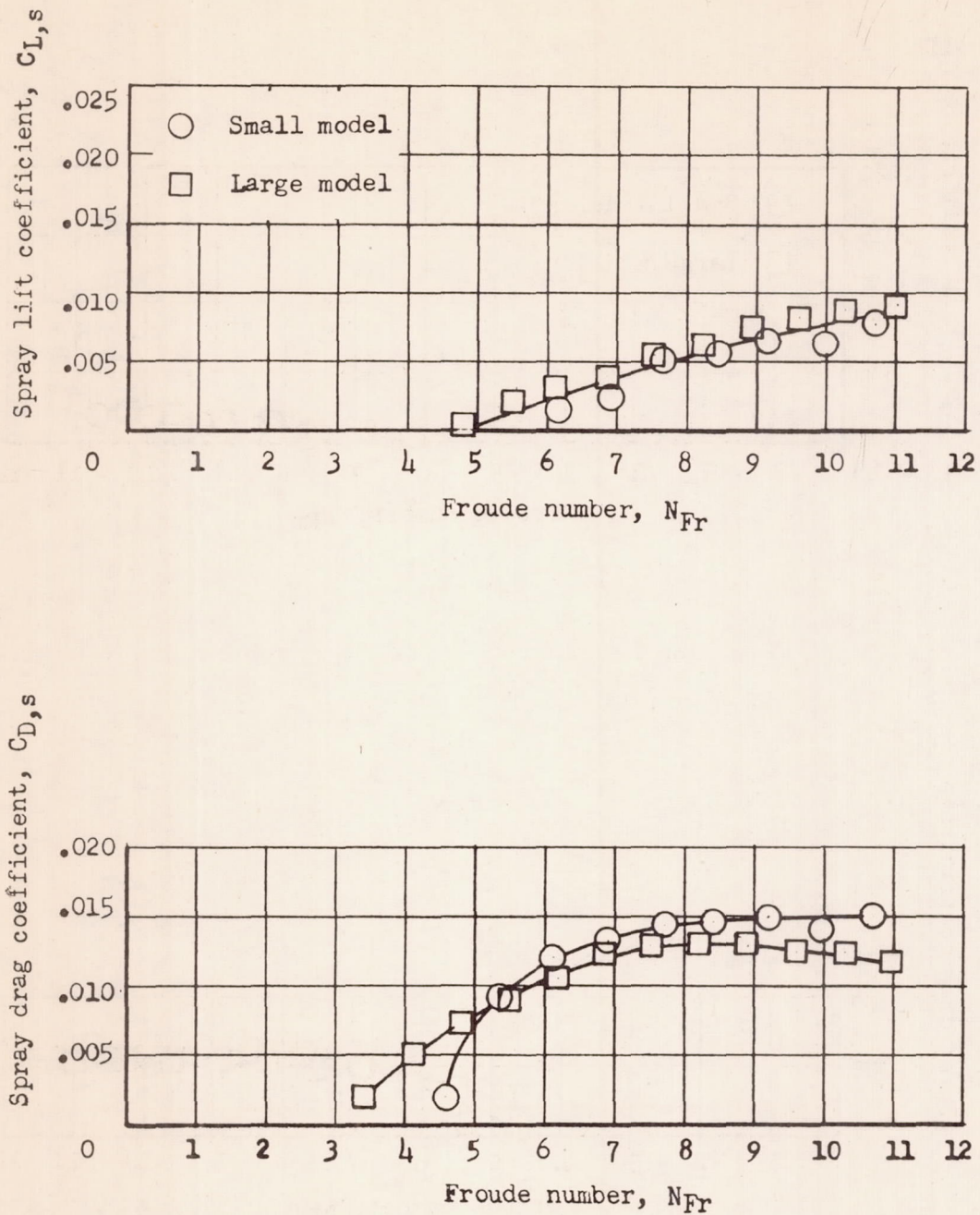
(a) Collector height, 1.0 beam.

Figure 10.- Variation of spray lift and drag coefficients with Froude number. $\tau = 9^\circ$; $l/b = 1.5$.



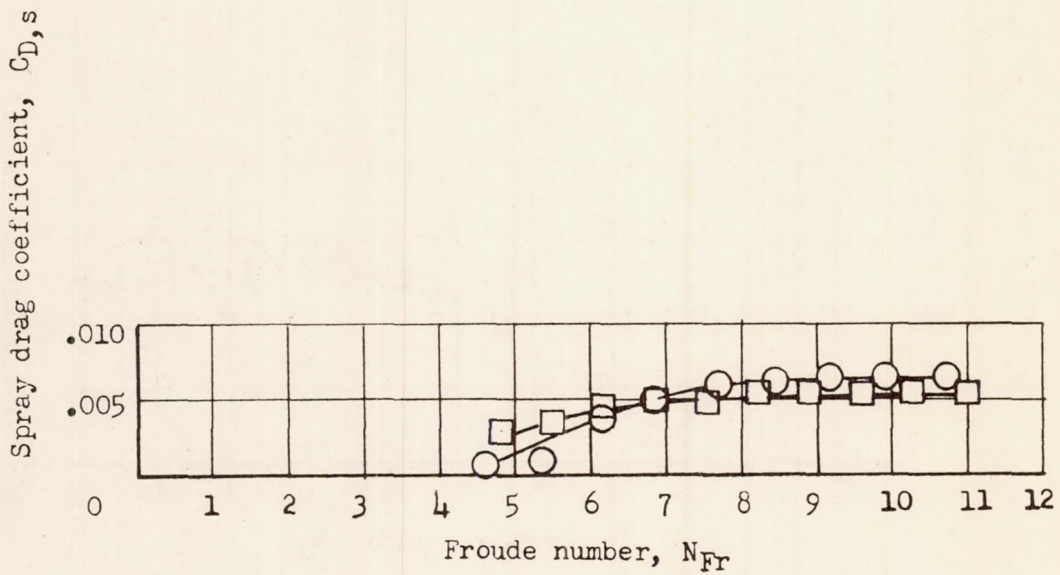
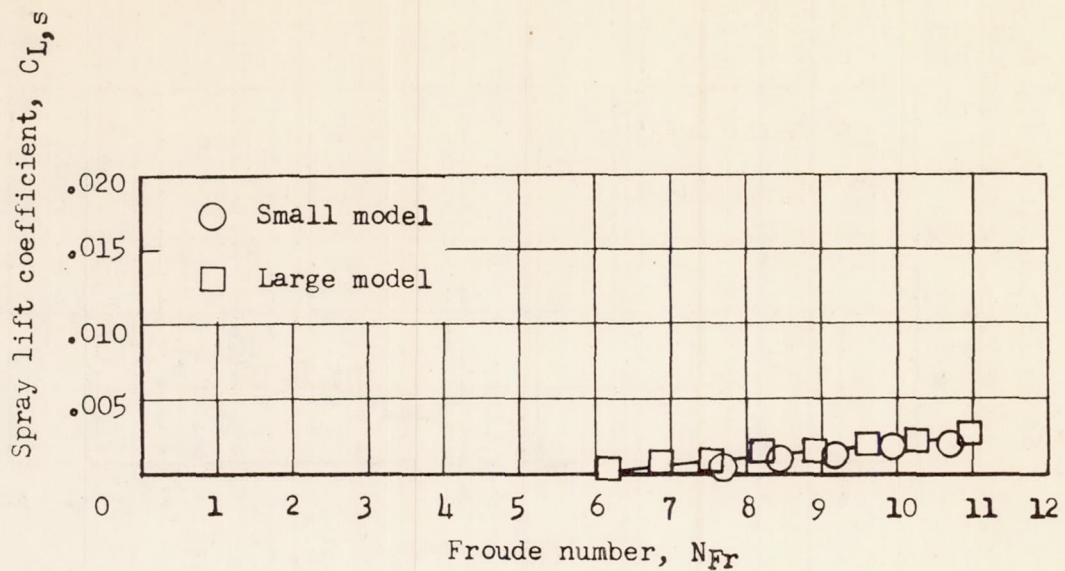
(b) Collector height, 1.5 beams.

Figure 10.- Concluded.



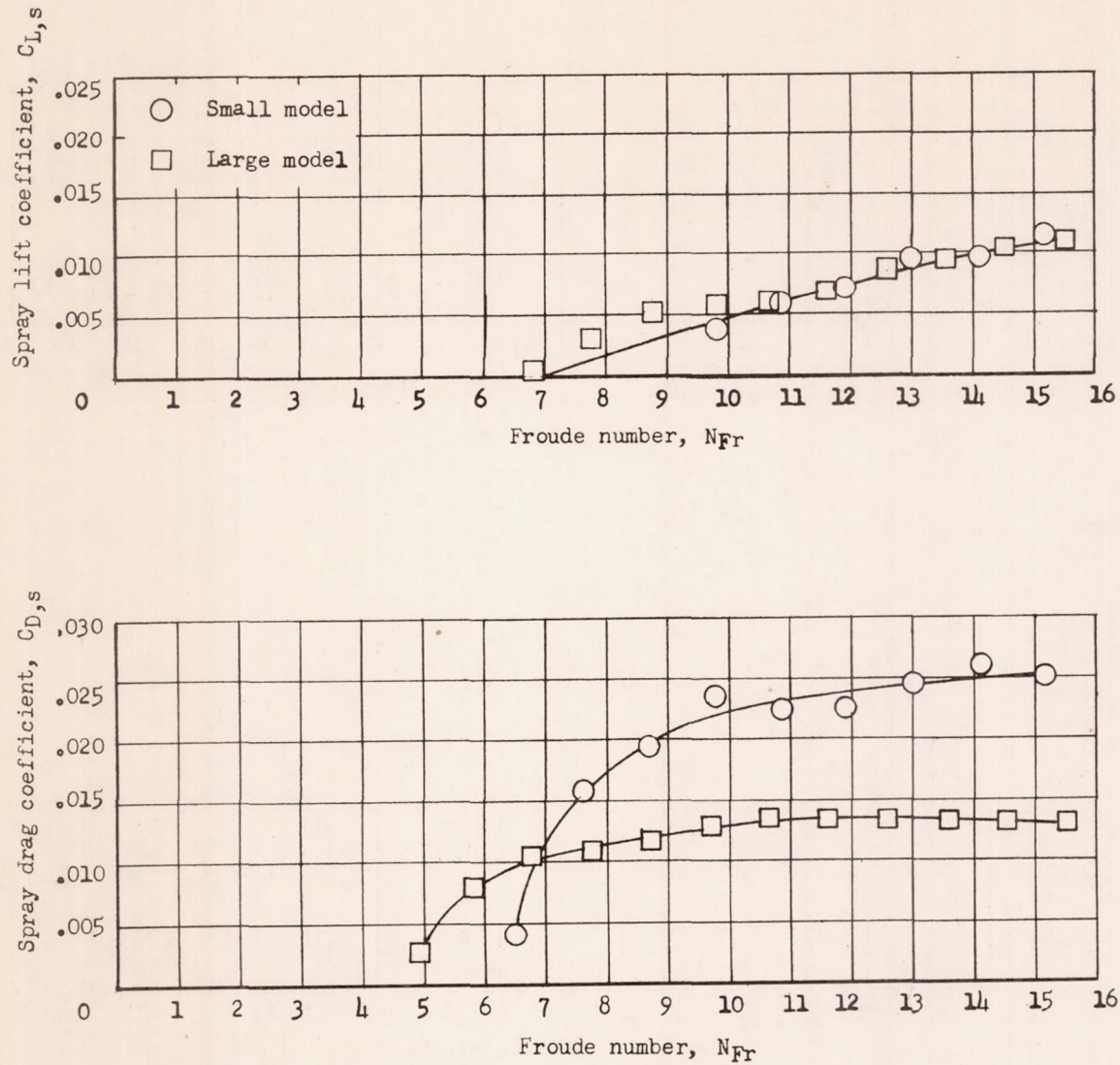
(a) Collector height, 1.0 beam.

Figure 11.- Variation of spray lift and drag coefficients with Froude number. $\tau = 90^\circ$; $l/b = 2.0$.



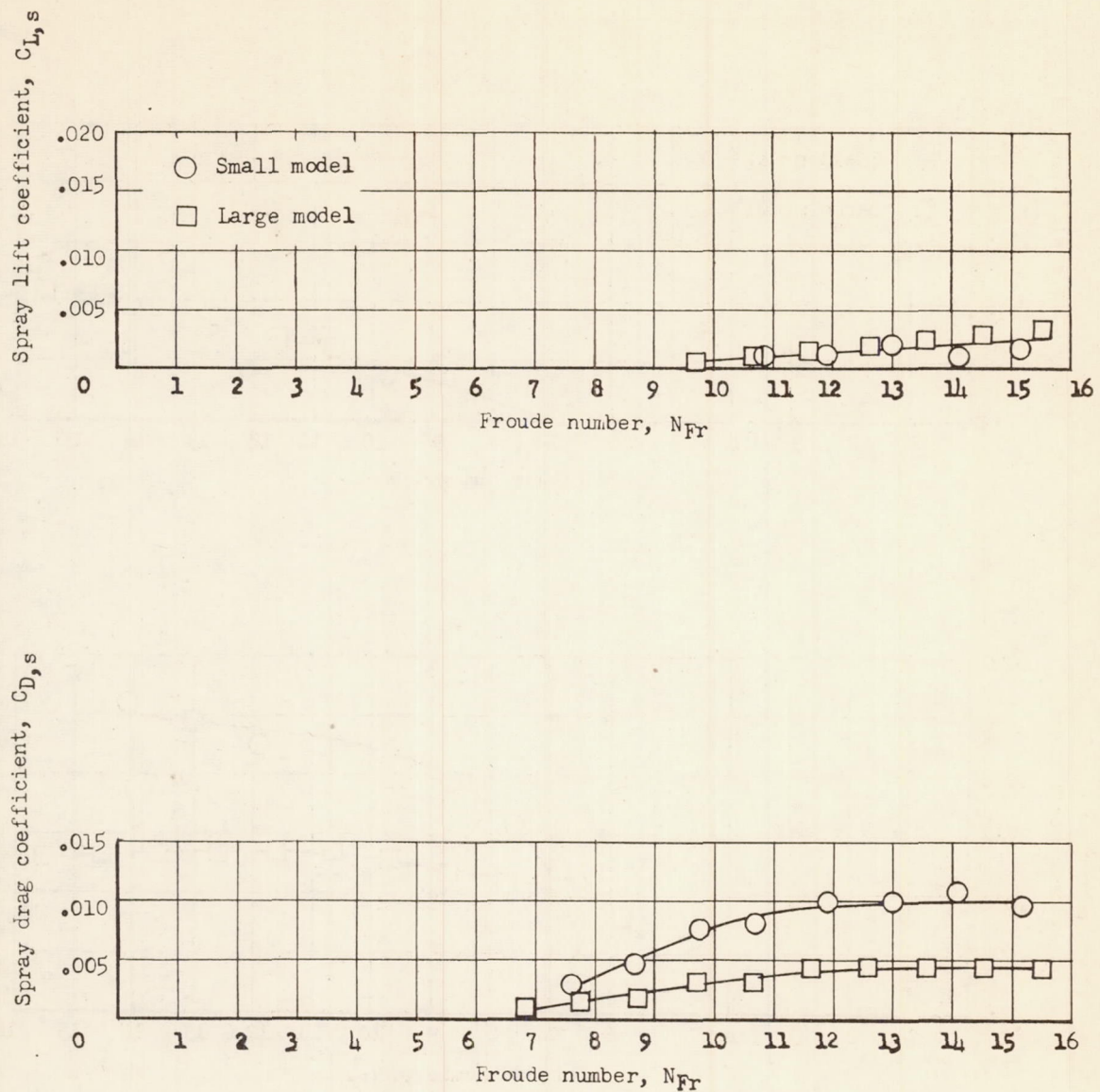
(b) Collector height, 1.5 beams.

Figure 11.- Concluded.



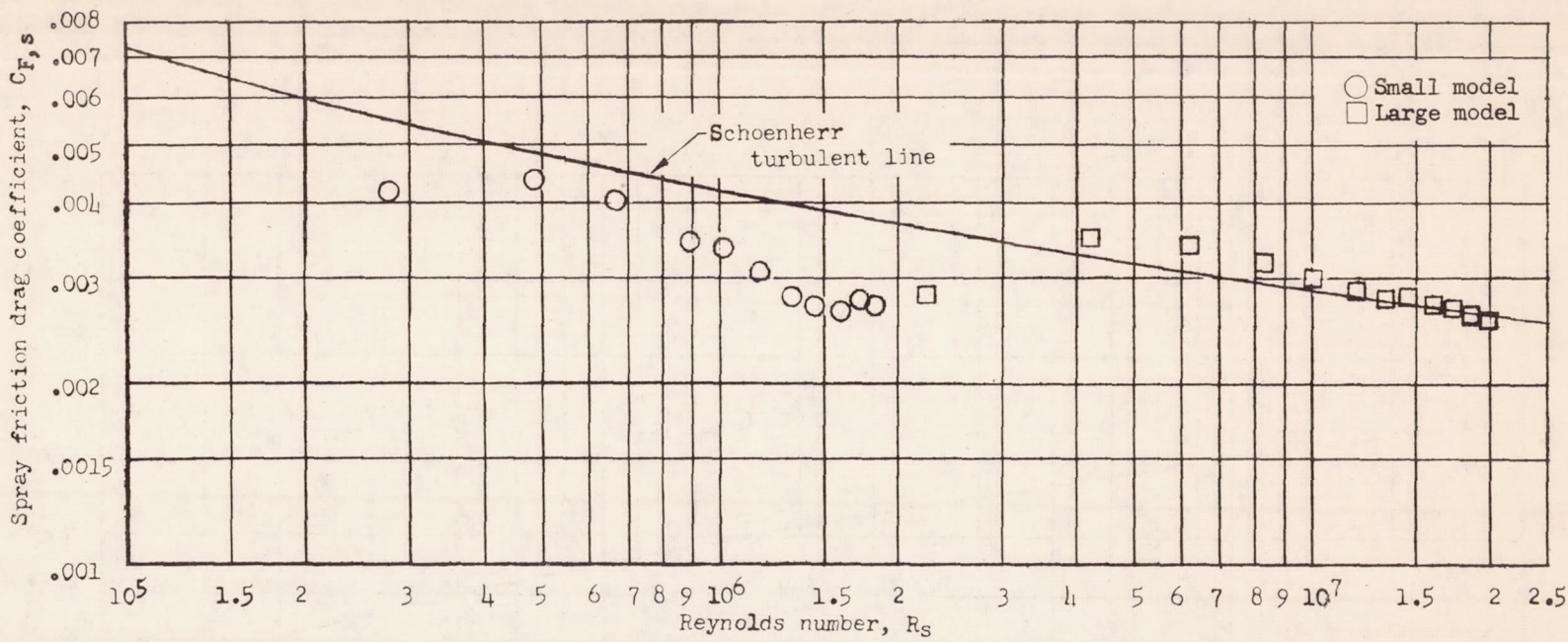
(a) Collector height, 1.0 beam.

Figure 12.- Variation of spray lift and drag coefficients with Froude number. $\tau = 9^\circ$; $l/b = 1.0$.



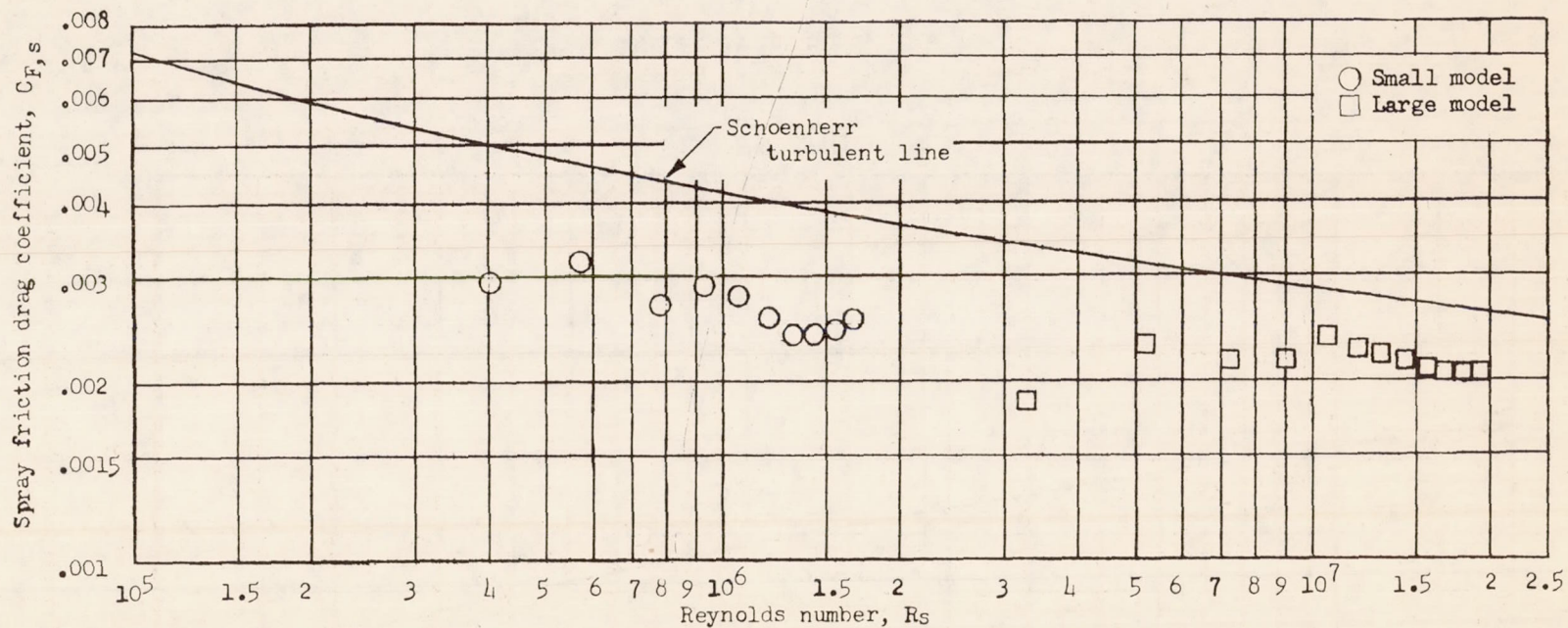
(b) Collector height, 1.5 beams.

Figure 12.- Concluded.



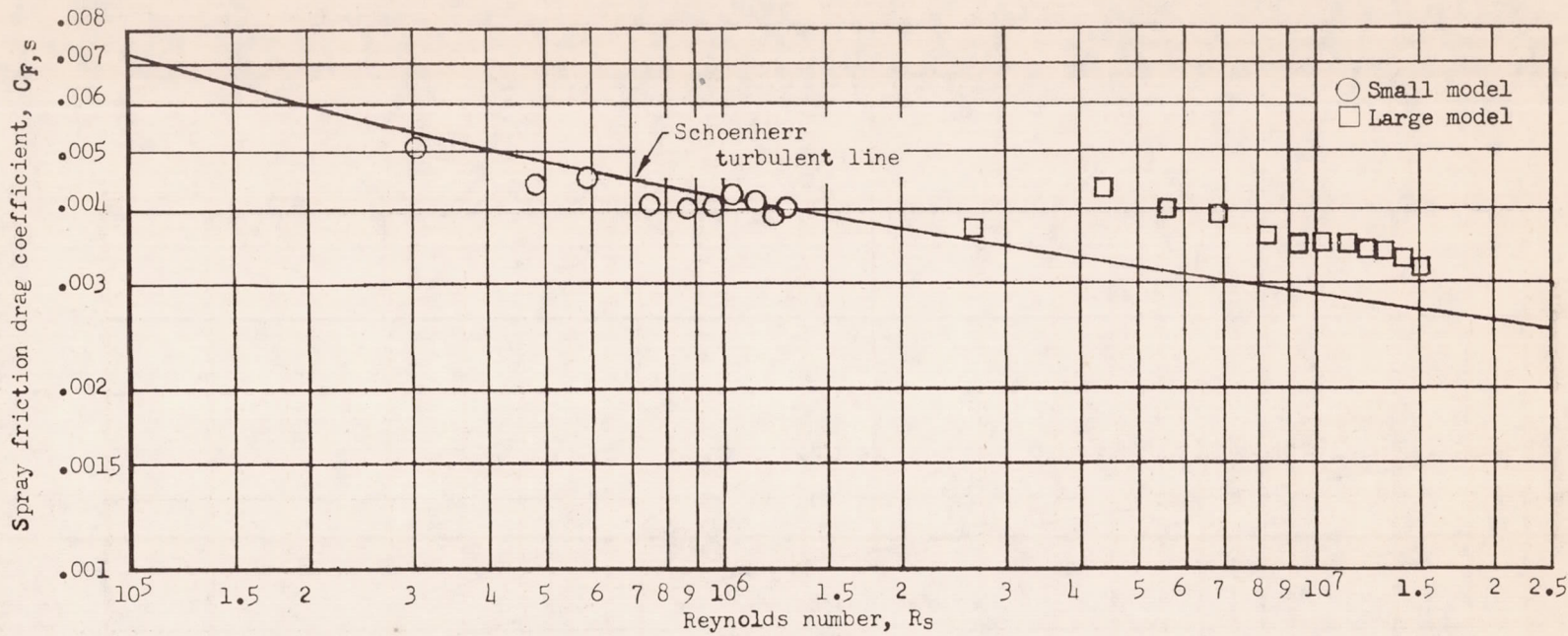
(a) Collector height, 1.0 beam.

Figure 13.- Variation of spray friction drag coefficient with Reynolds number. $\tau = 20^\circ$; $l/b = 1.5$.



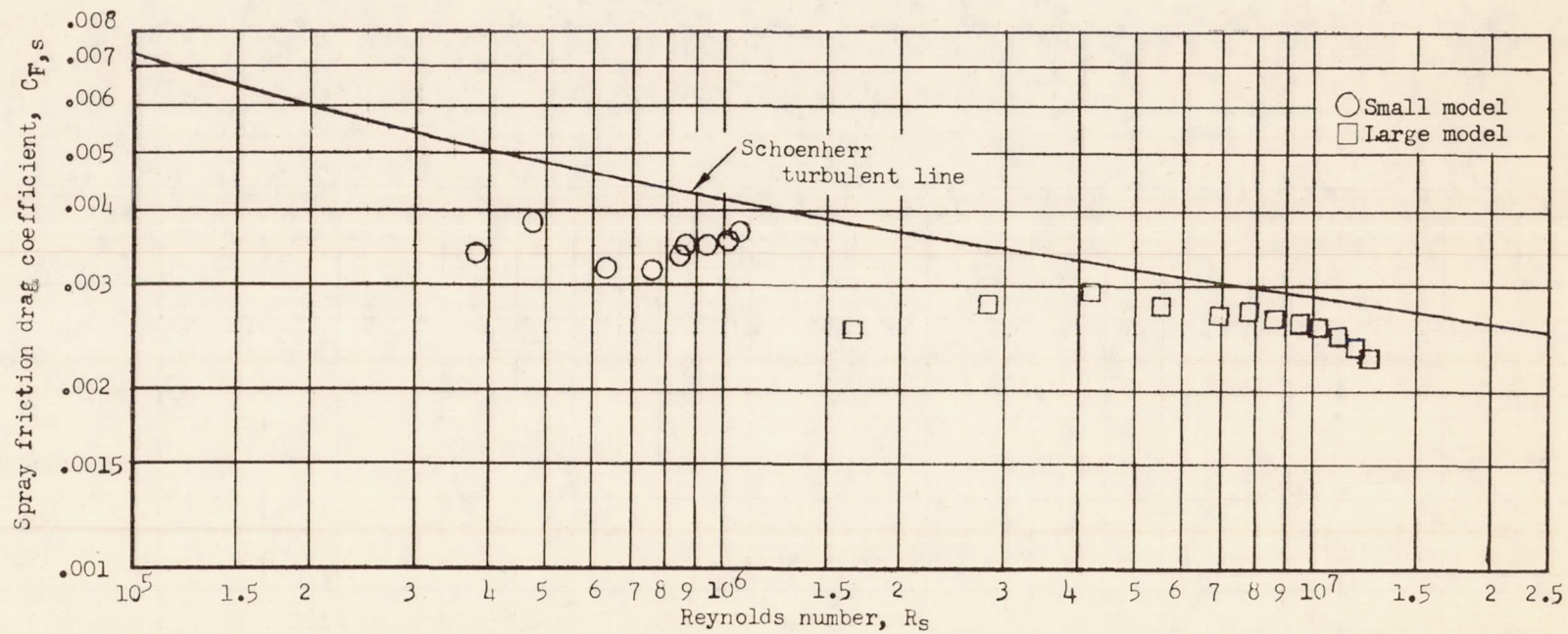
(b) Collector height, 1.5 beams.

Figure 13.- Concluded.



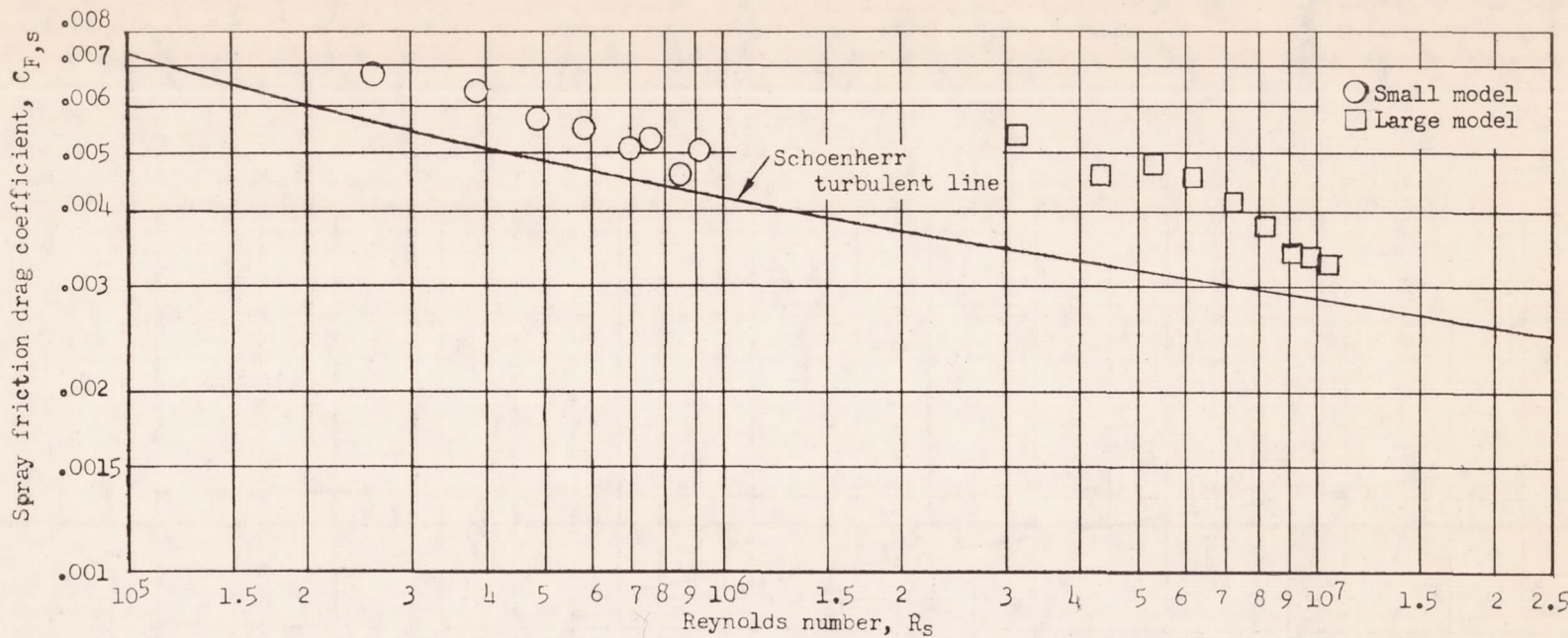
(a) Collector height, 1.0 beam.

Figure 14.- Variation of spray friction drag coefficient with Reynolds number. $\tau = 15^\circ$; $l/b = 1.5$.



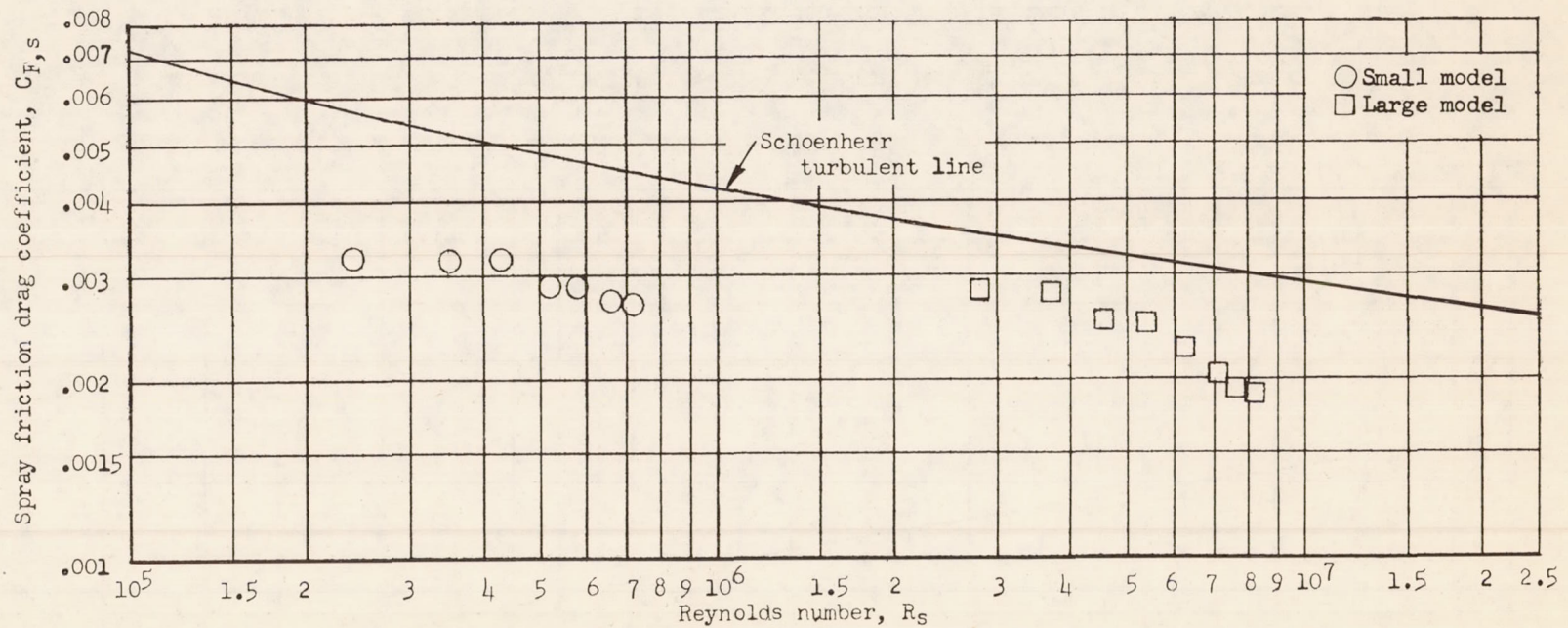
(b) Collector height, 1.5 beams.

Figure 14.- Concluded.



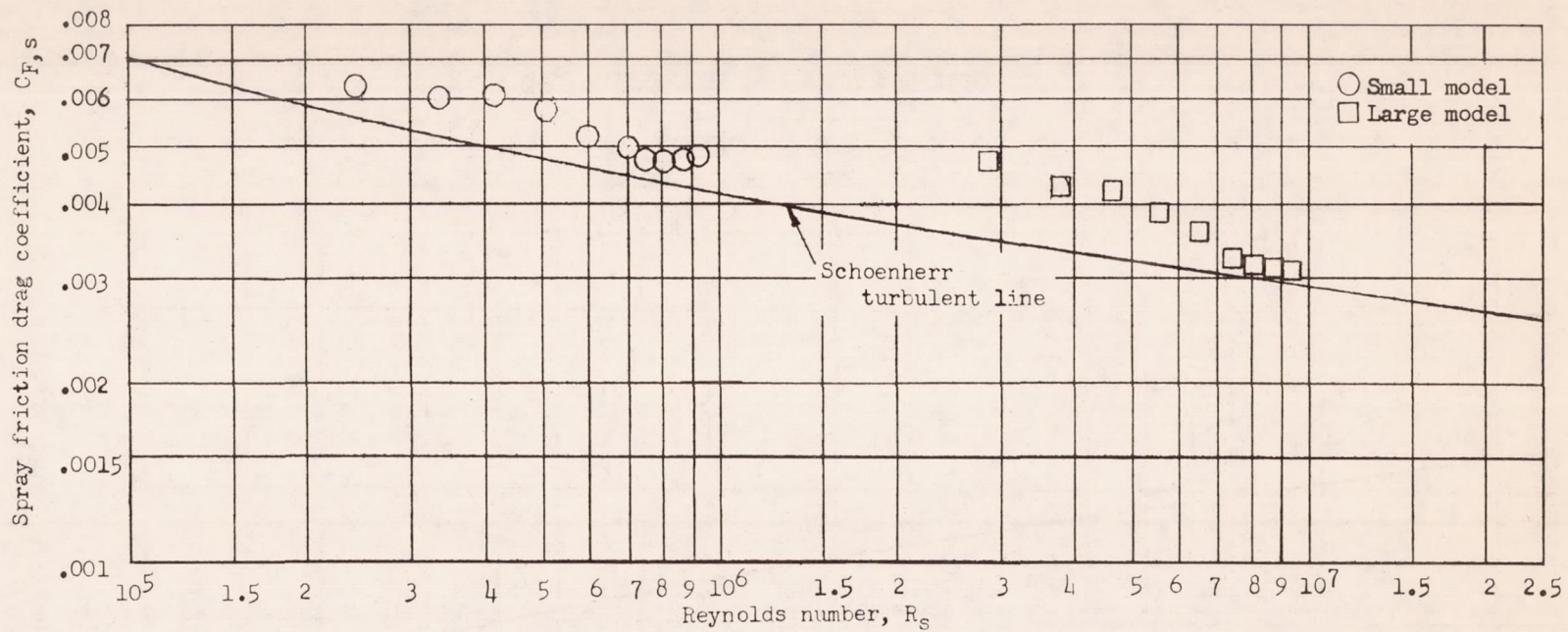
(a) Collector height, 1.0 beam.

Figure 15.- Variation of spray friction drag coefficient with Reynolds number. $\tau = 9^\circ$; $l/b = 2.0$.



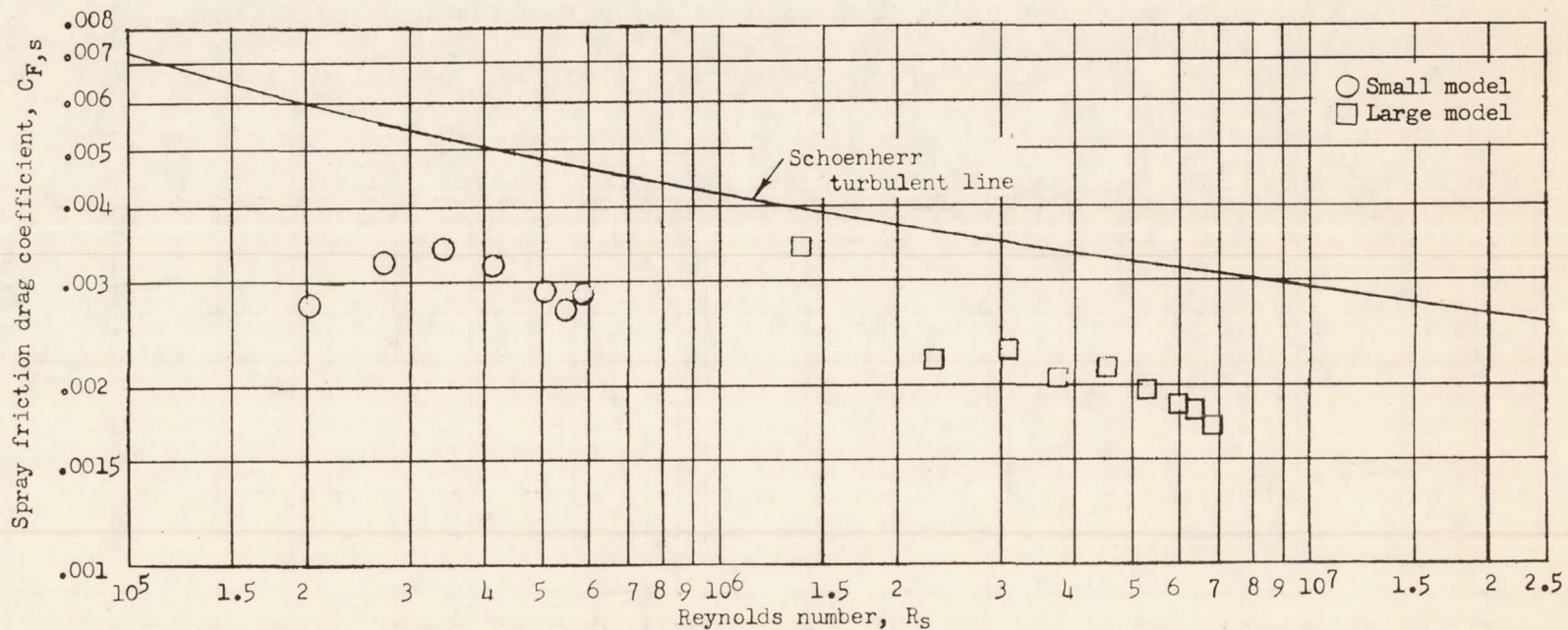
(b) Collector height, 1.5 beams.

Figure 15.- Concluded.



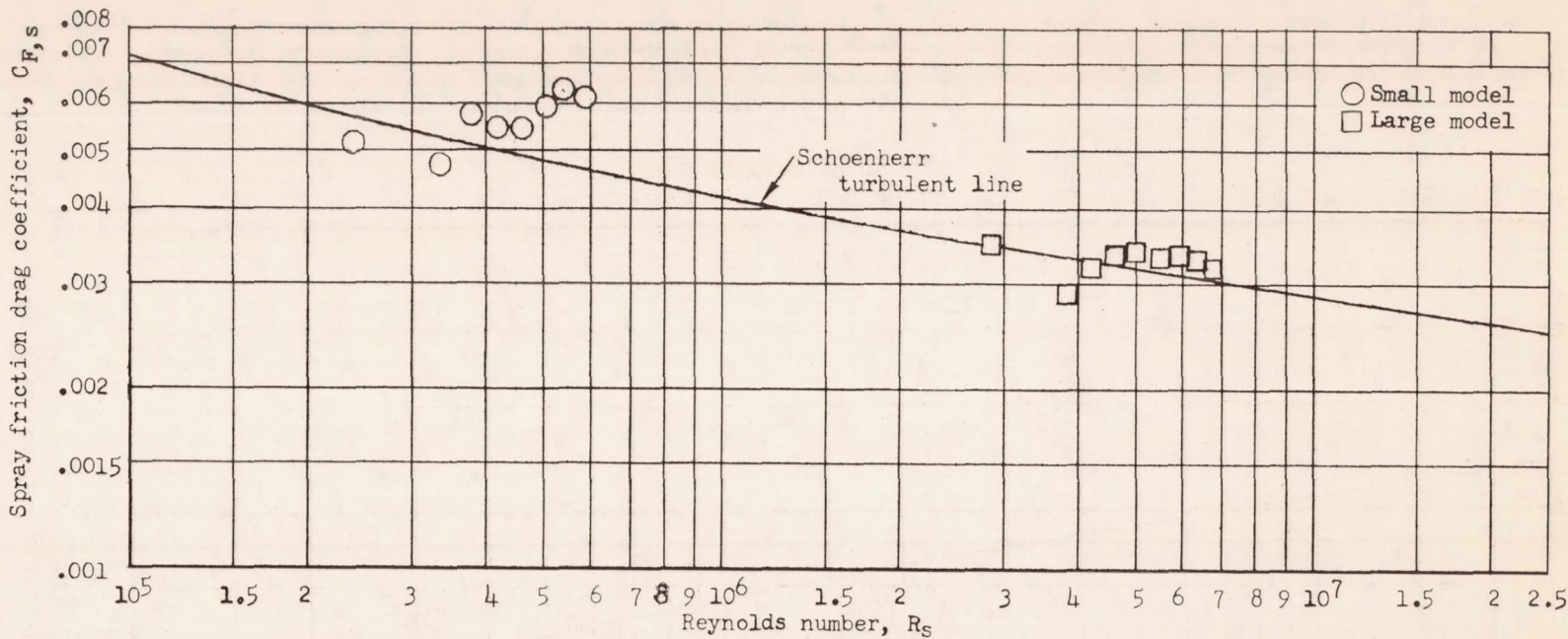
(a) Collector height, 1.0 beam.

Figure 16.- Variation of spray friction drag coefficient with Reynolds number. $\tau = 9^\circ$; $l/b = 1.5$.



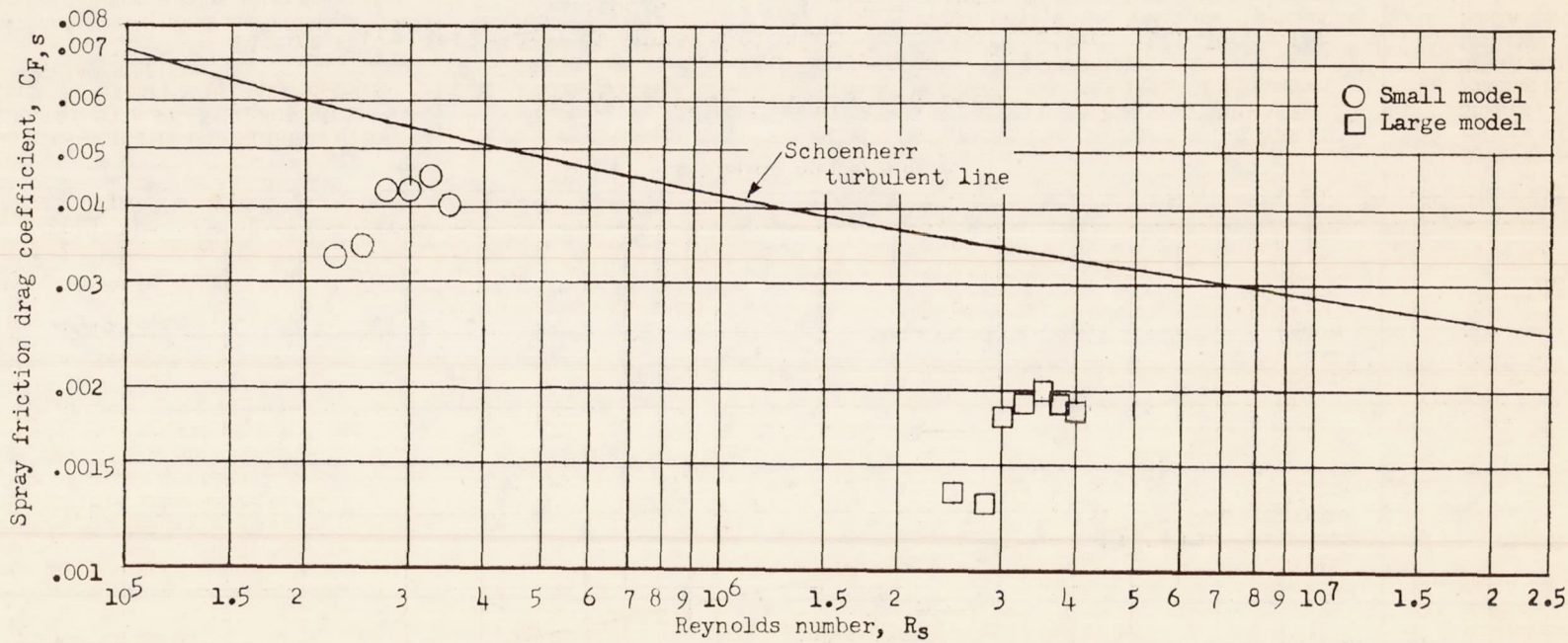
(b) Collector height, 1.5 beams.

Figure 16.- Concluded.



(a) Collector height, 1.0 beam.

Figure 17.- Variation of spray friction drag coefficient with Reynolds number. $\tau = 9^\circ$; $l/b = 1.0$.



(b) Collector height, 1.5 beams.

Figure 17.- Concluded.